NILS ANDERSEN AND PETER SIGMUND

ENERGY DISSIPATION BY HEAVY IONS IN COMPOUND TARGETS

Det Kongelige Danske Videnskabernes Selskab
Matematisk-fysiske Meddelelser **39**, 3

Kommissionær: Munksgaard
København 1974

Synopsis

We have studied theoretically the sharing of energy among the constituents of a polyatomic medium in random atomic collision cascades initiated by heavy atomic particles. Our main interest was to estimate the significance of possible nonstoichiometric effects as they might be of interest in radiation damage and sputtering.

It is assumed that primary and recoiling particles slow down by random collisions, scattering and stopping being described according to the framework of LINDHARD, SCHARFF, and coworkers. Collision cascades are characterized quantitatively by the recoil density and the slowing-down density. The former quantity specifies the number and energy distribution of recoil atoms of the various species in a cascade and is of particular interest in radiation damage problems. The latter quantity deals with the number and energy distribution of moving atoms in a stationary state and is of particular interest in sputtering problems. Both quantities are calculated for slowing-down in an infinite medium of uniform composition. We determine explicitly the asymptotic expressions at high ion energy as compared to the recoil energy. Deviations from this asymptotic behaviour are studied, too.

We find nonstoichiometric effects in both recoil and slowing-down density, and these effects are determined not only by different binding energies of different atomic species. A key role is being played by the mutual partial stopping cross sections of the constituent atoms of the medium. It turns out that deviations from stoichiometric behaviour are independent of concentration in case of the slowing-down density, but dependent on concentration in case of the recoil density.

A preliminary account of this work has been reported at a recent conference[0]).

PRINTED IN DENMARK
BIANCO LUNOS BOGTRYKKERI A/S
ISBN 87 7304 033 9

1. Introduction

When an ion beam hits a solid target, the kinetic energy of the ions is dissipated among the nuclei and electrons of the medium. This energy dissipation may result in a number of observable effects such as sputtering, disordering, ionization, dissociation, etc. The theory of energy dissipation in random and crystalline media has been developed in some detail, mostly for random, monatomic targets (for a recent review see, e.g., ref. 1). One of the central problems concerns the sharing of energy between the electrons and the nuclei of the system, i.e. the relative significance of atomic displacement effects (e.g. sputtering, disordering) on the one hand, and electronic excitation effects (e.g. photon and electron emission) on the other hand. According to theoretical predictions[2], this sharing of energy depends significantly on the atomic numbers and masses of the bombarding ion and the target atoms, and on the kinetic energy of the ion. When single crystals are bombarded, the sharing also depends on orientation[3].

In the present paper we deal with the sharing of energy between the different atomic species of a polyatomic random medium, with special emphasis being laid on *binary* compounds or alloys. By analogy with the sharing of energy between electrons and nuclei, one would expect, qualitatively, that the kinetic energy of a bombarding particle is not necessarily shared stoichiometrically between the different constituents of a polyatomic medium, i.e. that the sharing does not only depend on the composition, but also on the atomic masses involved. For example, in the limiting case of Rutherford scattering, it is easily seen that energy is dissipated preferentially among the *lightest* target nuclei, although even those, in this special case, receive several orders of magnitude less energy than what is dissipated among electrons.

When energy is deposited nonstoichiometrically, preferential displacement of one particular atomic species may result, and, moreover, composi-

tion changes may occur near the surface due to preferential sputtering. Most probably *neither effect is determined by energy sharing alone*, but an understanding of energy sharing is a basic requirement for further theoretical treatment of effects connected with different binding energies and mobilities of the atomic species.

Nonstoichiometric effects have been observed in sputtering[4-10]. Their occurrence appears to be well established, whilst very little systematics has yet developed from these studies. The interpretation will almost certainly be complicated in view of the fact that the sputtering yield of a binary material, according to experimental observation, may be significantly higher or lower than the sputtering yield of either of the pure materials[10-12]. Even rather small amounts of (alloyed or implanted) impurities may influence the sputtering yield significantly in either direction, dependent on the implanted species[13]. Surface topography appears to be a particularly important factor in determining the sputtering of alloyed targets[14, 15]. Systematic nonstoichiometric effects may be observed in experiments with single crystalline targets such as GaAs[16, 17]. In view of all these competing effects the present investigation is hardly more than one step forward on a rather long way towards a comprehensive understanding of the sputtering of compound targets.

While the theory of ion ranges in polyatomic targets is well developed[18-20], the theory of energy deposition in such targets, apart from a few early investigations of Frenkel-pair production[21-23] has concentrated on the gross spatial distribution of deposited energy[20, 24] and the overall sharing of energy between nuclei and electrons[24, 25]. In view of a lack of knowledge of atomic scattering cross sections, it was not possible in the early work on Frenkel-pair production[21-23] to arrive at quantitative criteria for the importance of nonstoichiometric effects in defect production. In fact, only the influence of different displacement threshold energies was considered in detail.

In this communication, we concentrate on random collision cascades mainly in diatomic solids, with the aim of estimating the relative and, less extensively, absolute numbers of recoiling or moving constituent atoms, mostly at keV bombarding ion energies where effects of nuclear stopping are most pronounced. Both with a view on potential applications, and in order to isolate possible nonstoichiometric effects, we are in particular interested in the case of *widely different masses* of the constituent atoms. This latter attitude is somewhat complementary to that of earlier investigators[21-23] while it is similar to that of Kistemaker et.al[26] who investigated energy dissipation in organic materials qualitatively.

The basic integral equations used in the analysis (sect. 2) are equivalent to those used before[23] in similar problems. The specific results are restricted, first to a special class of cross sections (sect. 3) and, second, to binary targets (sects. 4 and 6). The ternary case is considered briefly in sect. 5. We mainly consider asymptotic solutions for high ion energy as compared to the relevant recoil energies; in sect. 7 we briefly discuss the limitations to this approximation. In sect. 8 we discuss some physical implications and the relation to experimental results.

Electronic stopping is neglected in part of the analysis. This approximation restricts the energy range under consideration, but it will be shown that mostly *absolute* rather than *relative* numbers of moving atoms are affected by this simplification.

The presentation of the basic physical model will be kept brief. The reader who is less familiar with the notation and the way of argument is referred to ref. 1 for an introduction.

2. Basic Equations

Consider a random, infinite medium with $N_j = \alpha_j N$ atoms of type j (atomic number Z_j, atomic mass M_j) per unit volume. α_j $(0 \leq \alpha_j \leq 1;$ $\sum \alpha_j = 1)$ is the concentration of j-atoms, and N the atomic density [atoms/cm^3]. Let an atom of type i with initial energy E slow down in the medium.

For radiation damage calculations, we need the recoil density[27] $F_{ij}(E, E_0)$ which is defined as the average number of j-atoms *recoiling* per energy interval (E_0, dE_0) in a collision cascade initiated by an i-atom with initial energy E.

For sputtering calculations we need the slowing-down density[1, 28] $G_{ij}(E, E_0)$ which is the average number of j-atoms *moving* per energy interval (E_0, dE_0) in the stationary state, with ψ [i-atoms/sec] slowing down from energy E.

Following a well-known procedure[1], the following integral equations can be derived for F_{ij} and G_{ij},

$$\sum_k \alpha_k \int d\sigma_{ik} \{F_{ij} - F'_{ij} - F''_{kj}\} = \alpha_j \frac{d\sigma_{ij}(E, E_0)}{dE_0} \tag{1}$$

$$\sum_k \alpha_k \int d\sigma_{ik} \{G_{ij} - G'_{ij} - G''_{kj}\} = \frac{\psi}{N v_0} \delta_{ij} \delta(E - E_0) \tag{2}$$

where $F'_{ij} = F_{ij}(E', E_0)$ and $F''_{ij} = F_{ij}(E'', E_0)$, etc. Furthermore, E' and E'' are the energies of a scattered i-atom and a recoiling k-atom, respectively, after a collision that is governed by the differential cross section $d\sigma_{ik}(E, E', E'')$ The quantity v_0 is the velocity of a j-atom with energy E_0, and $d\sigma_{ij}(E, E_0)/dE_0$ stands for

$$\int_{E', E''} d\sigma_{ij}(E, E', E'')\delta(E'' - E_0).$$

The integral operators on the left-hand side of eqs. (1) and (2) are identical. However, eq. (2) has the form of an equation determining the *Green's function* of this integral operator. Hence, the functions F_{ij} and G_{ij} are interrelated in the following way,

$$F_{ij}(E, E_0) = \alpha_j \sum_l \int dE_1 \frac{N v_1}{\psi} G_{il}(E, E_1) \frac{d\sigma_{lj}(E_1, E_0)}{dE_0}. \tag{3}$$

Eq. (3) can be verified by insertion into eq. (1), interchanging the order of integrations, and utilizing eq. (2). Hence, once eq. (2) has been solved, F_{ij} follows from G_{ij} by integration according to (3). Both equations are equivalent to those used in ref. 23, although the present notation is more general. Furthermore, we use integral equations in the so-called "backward" form[29], while previous authors mostly used the forward form.

Eq. (2) will have to be solved subject to the boundary conditions

$$G_{ij}(E, E_0) = 0 \quad \text{for} \quad E < E_0. \tag{4}$$

In the special case of a *binary* medium, eq. (4) even holds for $E < E_0/\gamma_{ij}$ where

$$\gamma_{ij} = 4M_iM_j/(M_i + M_j)^2 \tag{5}$$

The following (usual) approximations will be made in order to solve eq. (2):

i) No binding energy is lost by recoiling atoms,*
ii) Electronic stopping is separated according to the scheme of LINDHARD et.al[2].

Then eq. (2) reads

$$\left.\begin{aligned} &\sum_k \alpha_k \int d\sigma_{ik}(E, T)\{G_{ij}(E, E_0) - G_{ij}(E - T, E_0) - G_{kj}(T, E_0)\} \\ &\quad + \sum_k \alpha_k S_{e,ik}(E) \frac{\partial}{\partial E} G_{ij}(E, E_0) = \frac{\psi}{N v_0} \delta_{ij} \delta(E - E_0) \end{aligned}\right\} \tag{2a}$$

* This simplification is dropped in appendix B.

where $S_{e,ik}(E)$ is the electronic stopping cross section for an i-atom colliding with a k-atom, and T the recoil energy. The cross section $d\sigma_{ik}(E, T)$ is that of *elastic* collisions.

It is most often possible to define an elastic-collision region[2] $E \lesssim E_c$ where electronic stopping is relatively small, so that it can be neglected as a first approximation. In this case we shall see (sects. 3, 4 and 5) that

$$G_{ij}(E, E_0) \sim g_j(E_0) \cdot E \quad \text{for} \quad E_0 \ll E \lesssim E_c \tag{6}$$

where $g_j(E_0)$ is a well defined function. The important features of eq. (6) are i) the linear dependence on E and ii) the nonoccurrence of the index i on the right-hand side.* From eqs. (2a) and (6) one verifies immediately that the following extension holds for higher energies beyond the elastic-collision region

$$G_{ij}(E, E_0) \sim g_j(E_0) \nu_i(E) \quad \text{for} \quad E_0 \ll E_c \quad \text{and} \quad E > E_c \tag{7}$$

where the $\nu_i(E)$ obey the set of equations

$$\sum_k \alpha_k \int d\sigma_{ik}(E, T) \{\nu_i(E) - \nu_i(E - T) - \nu_k(T)\} + \sum_k \alpha_k S_{e,ik}(E) \cdot \frac{d}{dE} \nu_i(E) = 0 \tag{8}$$

This is the generalization to polyatomic media of an integral equation first derived by LINDHARD et al.[2, 30]; a computer code for its solution has been worked out by WINTERBON[25]. It is obvious from eqs. (6) and (7) that, in order to determine deviations from stoichiometric energy sharing, we need the $g_j(E)$ function rather than $\nu_i(E)$. Since the former can be determined by solely considering the elastic-collision region, we shall restrict our attention to this region in the following sections. This simplifies the analysis substantially.

It may be stressed that the present argument is based on the *existence* of an elastic-collision region. For very different masses of constituent atoms, e.g. the case of a target containing very heavy atoms and *hydrogen* atoms, E_c may be prohibitively small. In such a case, caution has to be applied with respect to quantitative conclusions.

* $g_j(E_0)$ does, however, depend on *all* the constituents of the medium. See, e.g., eqs. (24a, b).

3. Power Cross Sections

The solution of integral equations of the type of eq. (2a) is facilitated greatly by use of a power cross section of the form[31]

$$d\sigma(E, T) = CE^{-m}T^{-1-m}dT; \; 0 \leq m < 1 \tag{9}$$

This cross section describes approximately the scattering of two Thomas-Fermi atoms over a limited range of energy E and recoil energy T. The proper value of m depends essentially on the product $E \cdot T$ and on the ion-target combination[31, 20]. At present, we apply eq. (9) in the form

$$d\sigma_{ij}(E, T) = C_{ij}E^{-m_i} \; T^{-1-m_i}dT; \; 0 \leq T \leq \gamma_{ij}E \tag{10}$$

in order to allow greatest possible generality within the inherent simplicity of the power cross section.* We note that eq. (10) is somewhat more general than the cross section used in ref. 23, since it allows for a variety of energy dependences of, e.g., the stopping power. We shall see below that this generalization is significant.

In sect. 6 we shall need more specified constants C_{ij}. We use the two forms

$$C_{ij} = \frac{\pi}{2} \cdot \lambda_{m_i} \cdot a_{ij}^2 \left(\frac{M_i}{M_j}\right)^{m_i} \left(\frac{2Z_i Z_j e^2}{a_{ij}}\right)^{2m_i}; \; m_i > \tfrac{1}{4}, \tag{10a}$$

and

$$C_{ij} = \frac{\pi}{2} \cdot \lambda_{m_i} \cdot a_{ij}'^2 \left(\frac{M_i}{M_j}\right)^{m_i} (2A_{ij}')^{2m_i}; \qquad m_i < \tfrac{1}{4}. \tag{10b}$$

The first choice[31] corresponds to Thomas-Fermi scattering with the screening radius

$$a_{ij} = 0.8853\, a_0 (Z_1^{2/3} + Z_2^{2/3})^{-1/2} \tag{11a}$$

and[31, 20]

$$\lambda_{1/2} = 0.327; \; \lambda_{1/3} = 1.309; \tag{11b}$$

The second choice[28] corresponds to exponential interaction with[32]

* Preferably one would use exponents m_{ij} instead of m_i; however, this would mean a substantial complication in the algebra. In fact, we have not succeeded in deriving eqs. (25) and (28) in this latter case, although the Laplace transform can be carried out easily. One might also suggest to use an index m_j. This would still be substantially more complicated than using m_i and, more important, would be physically a less reasonable choice than the one adopted in eq. (10).

$$\left.\begin{aligned} a'_{ij} &= \text{const.} = 0.219\ \text{Å}; \\ A'_{ij} &= 52(Z_i Z_j)^{3/4} eV; \end{aligned}\right\} \quad (11c)$$

and [28)]

$$\lambda_{0.055} = 15^*; \quad \lambda_0 = 24. \quad (11d)$$

Since we need mostly the cross sections at *low* particle energy E_0 (in the eV region) when calculating recoil and slowing-down densities[28, 34)], it is mostly the expressions (10b), (11c), and (11d) that will be used in applications. However, for low-mass ions – up to about oxygen – the Thomas-Fermi coefficients can be expected to be appropriate even in the lower eV-region, and will be used, therefore.

A convenient procedure of solving integral equations with a cross section like (9) has been described in detail by ROBINSON[33)] and one of the authors[1)] for the monatomic case. Straightforward generalization to the present situation is possible. Inserting $d\sigma_{ik}(E, T)$ as given by eq. (2a), setting $S_{e,ik}(E) = 0$, introducing the variables

$$E = E_0 e^u; \quad T = E_0 e^v,$$

following the procedure of ref. 1, and taking the Laplace transfrom with respect to the variable u yields

$$\tilde{G}_{ij}(s) \sum_k \beta_{ik}(s)\, \varepsilon_{ik}(s) - \sum_k \beta_{ik}(s)\, \tilde{G}_{kj}(s) = \frac{\psi E_0^{2m_i - 1}}{N v_0}\, \delta_{ij} \quad (12)$$

where

$$\beta_{ik}(s) = \frac{\gamma_{ik}^{s - m_i}}{s - m_i}\, \alpha_k\, C_{ik} \quad (13a)$$

and

$$\varepsilon_{ik}(s) = \frac{s - m_i}{\gamma_{ik}^{s - m_i}} \left[- \frac{\gamma_{ik}^{-m_i}}{m_i} - B_{\gamma_{ik}}(-m_i, s + 1) \right] \quad (13b)$$

$B_\gamma(x, y)$ is the incomplete beta function,

$$B_\gamma(x, y) = \int_0^\gamma dt\, t^{x-1} (1 - t)^{y-1} \quad (14)$$

and $\tilde{G}_{ij}(s)$ the Laplace transform

$$\tilde{G}_{ij}(s) = \int_0^\infty du\, e^{-su} G(E_0 e^u, E_0) \quad (15)$$

where use has been made of eq. (4).

* This value has been extracted from fig. 4 of ref. 28. It is rather uncertain. Note that for the high-energy portion of Born-Mayer interaction, a value about half as large was reported in ref. 28.

Eq. (12) is a system of algebraic equations that splits up into separate subsystems, one for each target element j. All the subsystems have the same determinant, but different inhomogeneities on the right-hand side.

In accordance with eq. (6), we are looking for solutions in the region $E \gg E_0$, i.e. large values of u. The procedure of determining asymptotic solutions is a generalization of the one described in detail in refs. 1,33,34. The main problem is to find the highest value of s, say $s = s_{ij}^{(0)}$ where $\tilde{G}_{ij}(s)$ has a single pole. Then, $G_{ij}(E, E_0)$ has the asymptotic form

$$G_{ij}(E, E_0) \sim A_{ij} \cdot (E/E_0)^{s_{ij}^{(0)}} \quad \text{for} \quad E \gg E_0 \tag{16}$$

where A_{ij} is the residuum of $\tilde{G}_{ij}(s)$ at $s = s_{ij}^{(0)}$. Some properties of the asymptotic expansion will be analysed in the following in the special case of a binary target. At present we discuss, somewhat loosely, some simple consequences of eq. (12).

Poles of $\tilde{G}_{ij}(s)$ may occur at the zeros of the determinant of eq. (12) and the poles of the subdeterminants. According to (13a, b) poles of subdeterminants might occur at $s = m_i$, and at some discrete negative values of s. The determinant, on the other hand, is expected to have a zero at $s = 1$, just as in the monatomic case. Indeed, from (13b), it follows that

$$\varepsilon_{ik}(1) = 1. \tag{17}$$

With this, the determinant achieves the form

$$D(1) = Det\{\delta_{ik} \sum_l \beta_{il}(1) - \beta_{ik}(1)\} \tag{18}$$

which is obviously zero. Moreover, it follows from (12) that

$$G_{ij}(s) \sim \tilde{G}_{kj}(s) \quad \text{for} \quad s \sim 1 \tag{19}$$

or, from (16), $A_{ij} = A_{kj}$. This proves eq. (6). The remaining problem is to calculate $g_j(E_0)$. This will be done by evaluating determinants.

In appendix A we prove that $s = s_{ij}^{(0)} = 1$ is the highest singularity for a general polyatomic target. This is not surprising from a physical point of view. It is evident already from eqs. (1) and (2) that energy conservation in binary collisions requires solutions that are asymptotically ($E \gg E_0$) linear in energy, and independent of the bombarding particle.

4. The Binary Case. I

With the abbreviation

$$B_j = \frac{\psi E_0^{2mj-1}}{N v_0} \tag{20}$$

the system of equations (12) has the solutions

$$\tilde{G}_{11}(s) = B_1 \frac{D_{11}^{(2)}}{D^{(2)}}; \quad \tilde{G}_{21}(s) = -B_1 \frac{D_{12}^{(2)}}{D^{(2)}} \tag{21}$$

where

$$D^{(2)} = [\beta_{11}(\varepsilon_{11} - 1) + \beta_{12}\varepsilon_{12}][\beta_{22}(\varepsilon_{22} - 1) + \beta_{21}\varepsilon_{21}] - \beta_{12}\beta_{21} \tag{22a}$$

$$D_{11}^{(2)} = \beta_{22}(\varepsilon_{22} - 1) + \beta_{21}\varepsilon_{21} \tag{22b}$$

$$D_{12}^{(2)} = -\beta_{21}. \tag{22c}$$

For $s = s_{ij}^{(0)} = 1$, and observing (17), we obtain

$$\tilde{G}_{11}(s) \sim \tilde{G}_{21}(s) \sim \frac{B_1 \beta_{21}(1)}{(s-1) D'(1)} \quad \text{for} \quad s \sim 1 \tag{23a}$$

where $D'(s) = \dfrac{d}{ds} D(s)$.*

Similarly, or by interchanging indices, we obtain

$$\tilde{G}_{22}(s) \sim \tilde{G}_{12}(s) \sim \frac{B_2 \beta_{12}(1)}{(s-1) D'(1)} \quad \text{for} \quad s \sim 1 \tag{23b}$$

Applying inverse Laplace Transform, we obtain asymptotic solutions

$$G_{11}(E) \sim G_{21}(E) \sim \frac{E}{E_0} \frac{B_1 \beta_{21}(1)}{D'(1)}; \quad \text{or} \quad g_1(E_0) = \frac{B_1 \beta_{21}(1)}{E_0 D'(1)} \tag{24a}$$

$$G_{22}(E) \sim G_{12}(E) \sim \frac{E}{E_0} \frac{B_2 \beta_{12}(1)}{D'(1)}; \quad \text{or} \quad g_2(E_0) = \frac{B_2 \beta_{12}(1)}{E_0 D'(1)}. \tag{24b}$$

These equations provide the connection with eq. (6).

* We drop the index $^{(2)}$ from $D^{(2)}$ for the rest of this section.

If we take the ratio of the fluxes of moving atoms of the two species, the determinant and the ion energy drop out, hence*

$$\left.\begin{aligned} &\frac{v_0 G_{11}(E)}{v_0 G_{12}(E)} \sim \frac{v_0 G_{21}(E)}{v_0 G_{12}(E)} \sim \frac{v_0 G_{11}(E)}{v_0 G_{22}(E)} \sim \frac{v_0 G_{21}(E)}{v_0 G_{22}(E)} \\ &\sim \frac{\alpha_1}{\alpha_2} \frac{\dfrac{\gamma_{21}^{1-m_2}}{1-m_2} C_{21} E_0^{1-2m_2}}{\dfrac{\gamma_{12}^{1-m_1}}{1-m_1} C_{12} E_0^{1-2m_1}} = \frac{\alpha_1 S_{21}(E_0)}{\alpha_2 S_{12}(E_0)} \end{aligned}\right\} \quad (25)$$

where

$$S_{ik}(E) = \int_0^{\gamma_{ik}E} T d\sigma_{ik}; \quad \beta_{ik}(1) = \alpha_k S_{ik}(E) E_0^{2m_i - 1}; \quad (26)$$

$S_{ik}(E)$ is the nuclear stopping cross section of an i-atom colliding with a k-atom.

Next, we insert eq. (24a, b) into eq. (3), and evaluate F_{ij} to the highest power of E/E_0, i.e. the linear term. This yields, in the same notation as eq. (24),

$$F_{11}(E) \sim F_{21}(E) \sim \frac{E}{E_0^2} \frac{\beta_{21}(1)(\beta_{11}(1) + \beta_{12}(1))}{D'(1)} \quad (27a)$$

$$F_{22}(E) \sim F_{12}(E) \sim \frac{E}{E_0^2} \frac{\beta_{12}(1)(\beta_{22}(1) + \beta_{21}(1))}{D'(1)} \quad (27b)$$

From this we obtain the ratio

$$\frac{F_{11}(E)}{F_{22}(E)} \sim \frac{\alpha_1 S_{21}(E_0)}{\alpha_2 S_{12}(E_0)} \frac{\alpha_1 S_{11}(E_0) + \alpha_2 S_{12}(E_0)}{\alpha_2 S_{22}(E_0) + \alpha_1 S_{21}(E_0)} \quad (28)$$

where again eq. (26) has been used. Eqs. (25) and (28) show that in general

i) the ratio of the fluxes of moving 1-atoms to moving 2-atoms is proportional to the ratio of the respective concentrations, but not nessecarily identical with it, and

ii) an even more pronounced deviation from stoichiometry is expected in the ratio of the number of recoiling 1-atoms and recoiling 2-atoms, since the concentrations enter nonlinearly.

* We include the velocity v_0 in $v_0 G_{ij}(E, E_0)$ because of the index j in $v_0 = \sqrt{2E_0/M_j}$. Note that both in sputtering theory[28] and in eq. (3) it is actually *this* product that is important.

5. The Ternary Case

We briefly mention the asymptotic solutions for the case of a ternary compound. From (12) we obtain.

$$G_{11} \sim G_{21} \sim G_{31} \sim B_1 \frac{D_{11}^{(3)}}{D^{(3)\prime}} \frac{E}{E_0} \tag{29a}$$

$$G_{12} \sim G_{22} \sim G_{32} \sim B_2 \frac{D_{22}^{(3)}}{D^{(3)\prime}} \frac{E}{E_0} \tag{29b}$$

$$G_{13} \sim G_{23} \sim G_{33} \sim B_3 \frac{D_{33}^{(3)}}{D^{(3)\prime}} \frac{E}{E_0} \tag{29c}$$

where

$$D_{11}^{(3)} = \beta_{21}\beta_{31} + \beta_{21}\beta_{32} + \beta_{23}\beta_{31} \tag{30a}$$

$$D_{22}^{(3)} = \text{cycl. perm.} \tag{30b}$$

$$D_{33}^{(3)} = \text{cycl. perm.} \tag{30c}$$

$$D^{(3)\prime} = \frac{d}{ds} D^{(3)}(s)\big|_{s=1} = (\beta_{11}\varepsilon'_{11} + \beta_{12}\varepsilon'_{12} + \beta_{13}\varepsilon'_{13}) D_{11}^{(3)} + \text{cycl. perm.}, \tag{31}$$

and the upper index (3) indicates the ternary case. Both $D_{ik}^{(3)}$, ε'_{ik}, and β_{ik} are taken at $s = 1$. The B_i are given in eq. (20). It is straightforward to determine *relative* magnitudes of the G_{ik} from eqs. (29–31).

By applying eq. (3) to the ternary case, we readily obtain

$$F_{11} \sim F_{21} \sim F_{31} \sim \frac{E}{E_0^2} \frac{\beta_{11} D_{11}^{(3)} + \beta_{21} D_{22}^{(3)} + \beta_{31} D_{33}^{(3)}}{D^{(3)\prime}} \tag{32a}$$

$$F_{12} \sim F_{22} \sim F_{32} \sim \frac{E}{E_0^2} \frac{\beta_{12} D_{11}^{(3)} + \beta_{22} D_{22}^{(3)} + \beta_{32} D_{33}^{(3)}}{D^{(3)\prime}} \tag{32b}$$

$$F_{13} \sim F_{23} \sim F_{33} \sim \frac{E}{E_0^2} \frac{\beta_{13} D_{11}^{(3)} + \beta_{23} D_{22}^{(3)} + \beta_{33} D_{33}^{(3)}}{D^{(3)\prime}} \tag{32c}$$

Evaluation of G_{ik} and F_{ik} in terms of stopping powers can be made by use of eqs. (35) and (26). We shall not go into any further details with the general ternary case.

6. The Binary Case. II

In this section we discuss in more detail some implications of the equations derived in sect. 4 for the binary case. For illustration we have evaluated numerically the solutions in a few specific cases.

Let us first consider the ratio between the slowing-down densities. Eq. (25) may be written

$$\frac{v_0 G_1}{v_0 G_2} \sim \frac{\alpha_1}{\alpha_2} \cdot \frac{C_{21}}{C_{12}} \cdot X \cdot E_0^{2(m_1 - m_2)}, \tag{25a}$$

where the constant

$$X = \frac{1 - m_1}{1 - m_2} \gamma^{m_1 - m_2}$$

is of the order of one (In view of eq. (6), we dropped the *first* index from G_{ij}). For strictly stoichiometric behaviour, we would just have α_1/α_2 on the right-hand side of eq. (25a). If $m_1 \neq m_2$, the ratio (25a) depends on the energy E_0, and in such a way that the fraction of moving atoms of the *lighter* species increases in the *upper* parts of the energy spectrum. If $m_1 = m_2 \equiv m$, (25a) reduces to

$$\frac{v_0 G_1}{v_0 G_2} \sim \frac{\alpha_1}{\alpha_2} \cdot \frac{C_{21}}{C_{12}} = \frac{\alpha_1}{\alpha_2} \left(\frac{M_2}{M_1} \right)^{2m}, \tag{25b}$$

according to eqs. (10a, b). Then the deviation from stoichiometry does not vary over the energy spectrum (for $E_0 \ll E$) and is determined solely by the mass ratio and m. Since $m \geq 0$, the lighter species dominates at those energies where (25b) is valid.

The ratio between the recoil densities, eq. (28), is energy-independent even for $m_1 \neq m_2$, as may be seen by inserting

$$S_{ik}(E_0) = \frac{C_{ik}}{1 - m_i} \gamma^{1 - m_i} E_0^{1 - 2m_i}$$

into eq. (28),

$$\frac{F_1}{F_2} \sim \frac{\alpha_1}{\alpha_2} \cdot \frac{\alpha_1 \cdot \gamma^{m_1 - 1} \cdot \dfrac{C_{11}}{C_{12}} + \alpha_2}{\alpha_2 \cdot \gamma^{m_2 - 1} \cdot \dfrac{C_{22}}{C_{21}} + \alpha_1} = \frac{\alpha_1}{\alpha_2} \cdot Y \tag{28a}$$

where again the *first* index was dropped from F_{ij}. Here the factor Y depends on concentration, and its variation with α_1 and α_2 determines the deviation

from stoichiometry. For small amounts of one of the constituents, (28a) reduces to

$$\frac{F_1}{F_2} \sim \frac{\alpha_1}{\alpha_2} \cdot \frac{S_{11}(E_0)}{S_{12}(E_0)} = \frac{\alpha_1}{\alpha_2} \cdot \frac{C_{11}}{C_{12}} \gamma^{m_1 - 1} (\alpha_2 \ll 1) \tag{28b}$$

$$\frac{F_1}{F_2} \sim \frac{\alpha_1}{\alpha_2} \cdot \frac{S_{21}(E_0)}{S_{22}(E_0)} = \frac{\alpha_1}{\alpha_2} \cdot \frac{C_{21}}{C_{22}} \gamma^{1 - m_2} (\alpha_1 \ll 1). \tag{28c}$$

A useful dimensionless quantity in the calculation of the average number N_i of *displaced* i-atoms is the displacement effiency[33] K_i, defined by*

$$N_i = \int_{E_{d,i}}^{\infty} F_i(E, E_0)\, dE_0 = \frac{E}{E_{d,i}} \cdot \alpha_i \cdot K_i \tag{33}$$

$E_{d,i}$ is the displacement threshold energy for atoms of type i. In the monatomic case one obtains[27]

$$K = \frac{m}{\psi(1) - \psi(1 - m)}, \tag{34}$$

i.e. $0 \leq K \leq \dfrac{6}{\pi^2}$ for $0 \leq m \leq 1$.

For the numerical examples, we have chosen binary compounds of rather different masses : Tungsten Oxide ($\gamma = 0.295$), Uranium Carbide ($\gamma = 0.183$), and Copper-Gold ($\gamma = 0.738$). In the calculations we have used the two values of m, 0.055, eq. (11d) and 0.333, eq. (11b). Both choices $m_1 \neq m_2$ and $m_1 = m_2$ have been considered. In the case of different m-values, $m = 0.333$ has been used for the lighter element, and $m = 0.055$ for the heavier one.

According to eq. (24), the slowing-down density G_i is determined by an equation of the form

$$\frac{N v_0}{\psi E} \cdot G_i = E_0^{2(m_i - 1)} \cdot A_i ; \; E_0 \ll E. \tag{35}$$

Figs. 1a and 1b show the energy dependence of this quantity for W and O in W–O compounds, plotted for concentration 0, 1/4, 1/2, 3/4 and 1, in

* The present model for the displacement number is oversimplified, since it does not take into account replacement events. Therefore, the displacement efficiency can become greater than 0.5, contrary to the result of ref. 33. Although replacements constitute another interesting aspect of collision cascades in polyatomic targets, we refrain from including them here, since the available models seem to be even less quantitative than those for displacement. In particular, no experimental data are known to us for replacement threshold energies for any system.

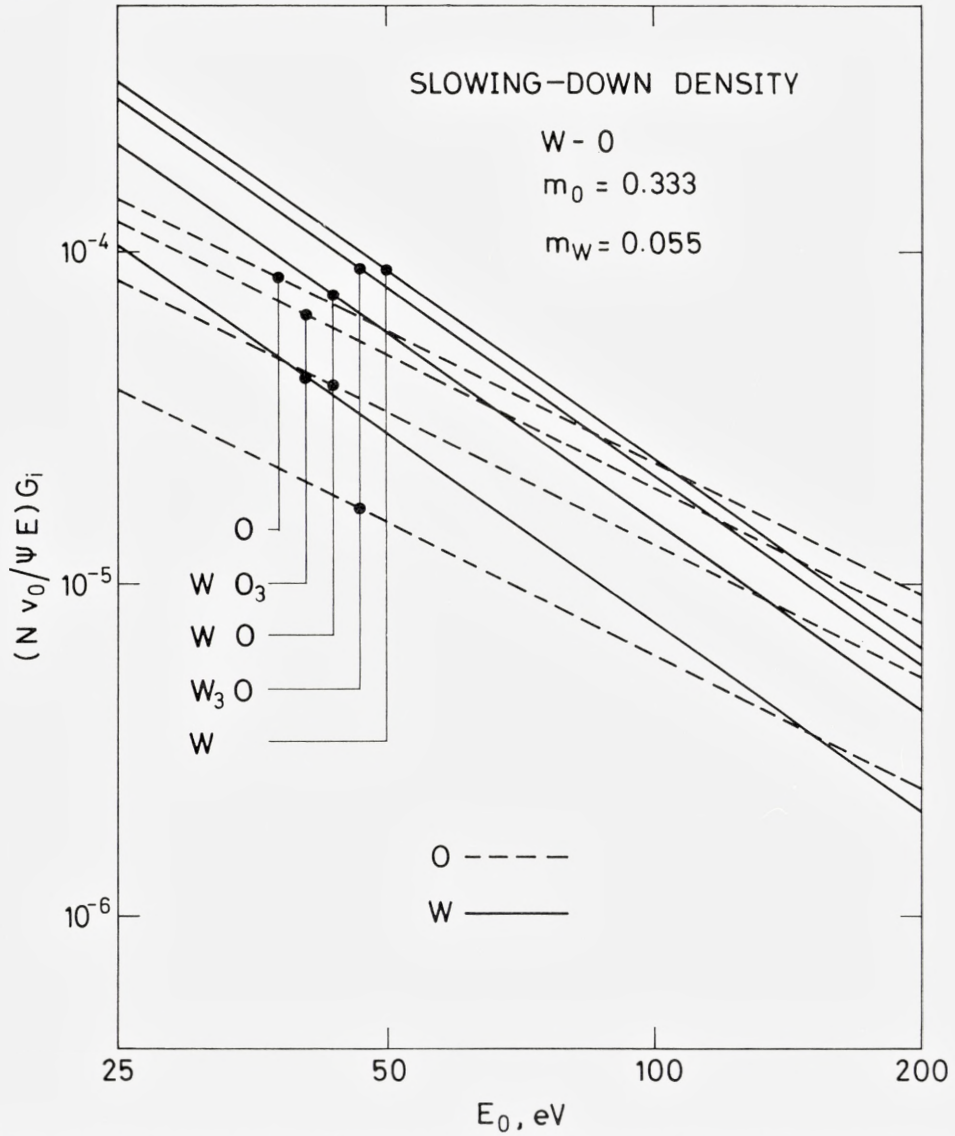

Fig. 1. Slowing-down densities of each of the two constituents of three binary compounds in relative units, eq. (35), as a function of spectral energy E_0. Parameters m_O, m_W, etc. refer to the scattering law, eq. (10). Note the different energy dependences of the spectra in case of $m_1 \neq m_2$. Full-drawn and stipled lines refer to the heavy and light constituent, respectively.

Fig. 1a. Tungsten oxide, $m_O > m_W$.

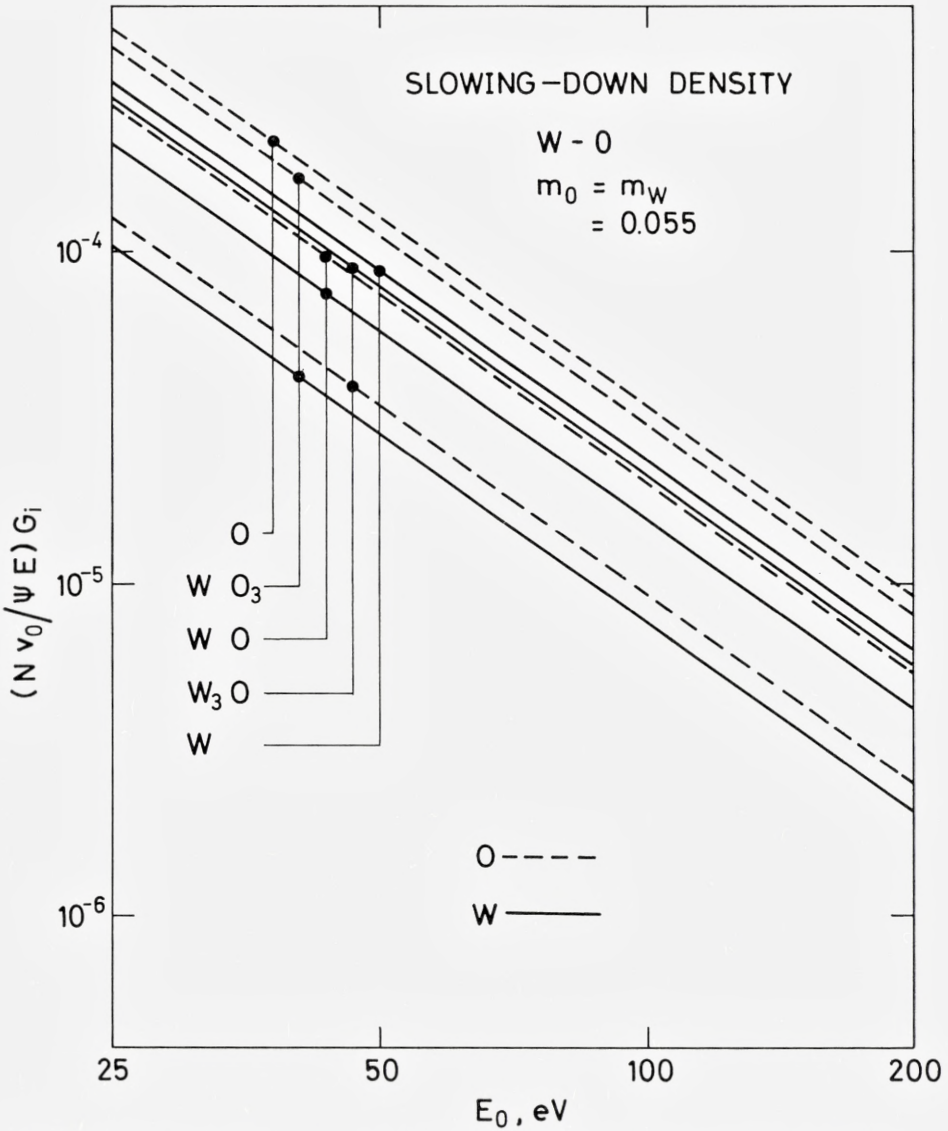

Fig. 1b. Tungsten oxide, $m_O = m_W$; this graph is presumably less realistic than fig. 1a.

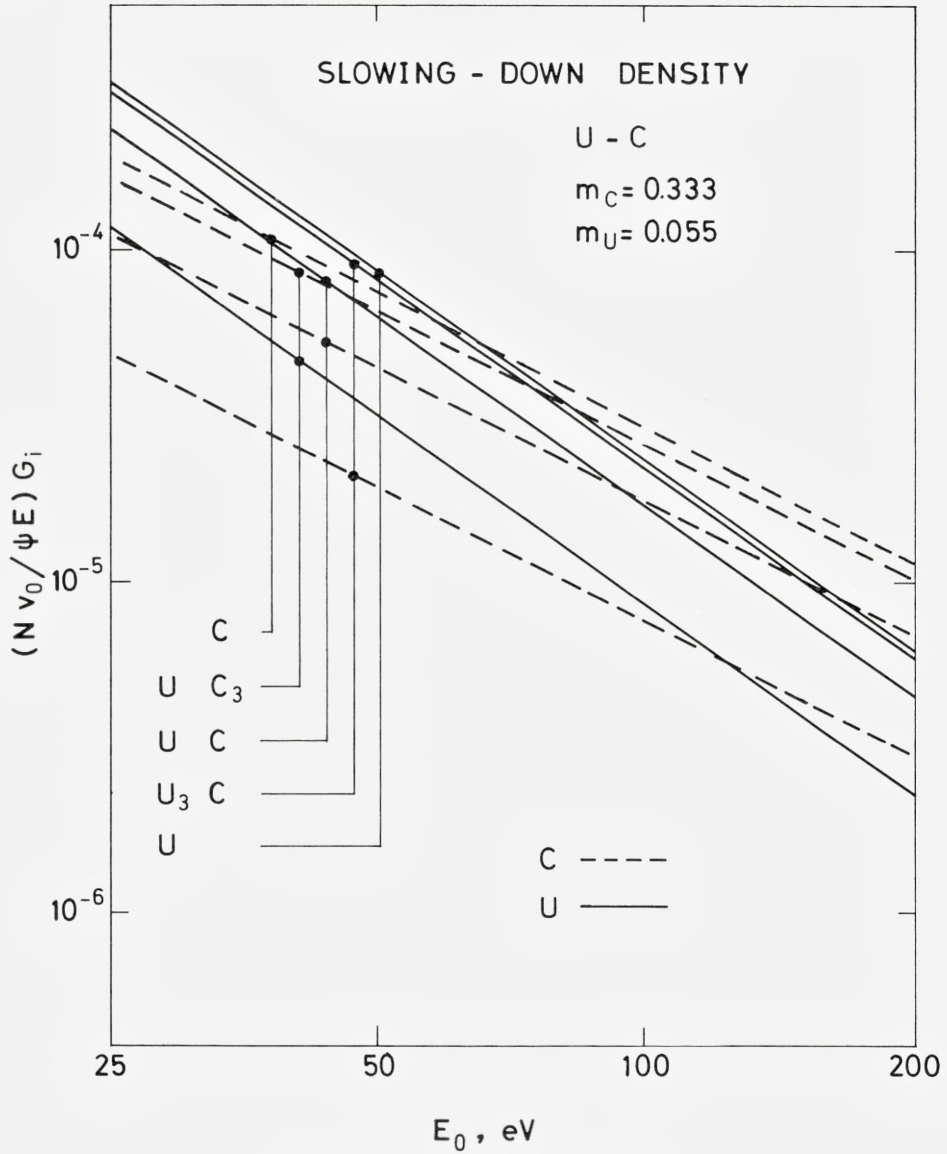

Fig. 1c. Uranium carbide, $m_C > m_U$.

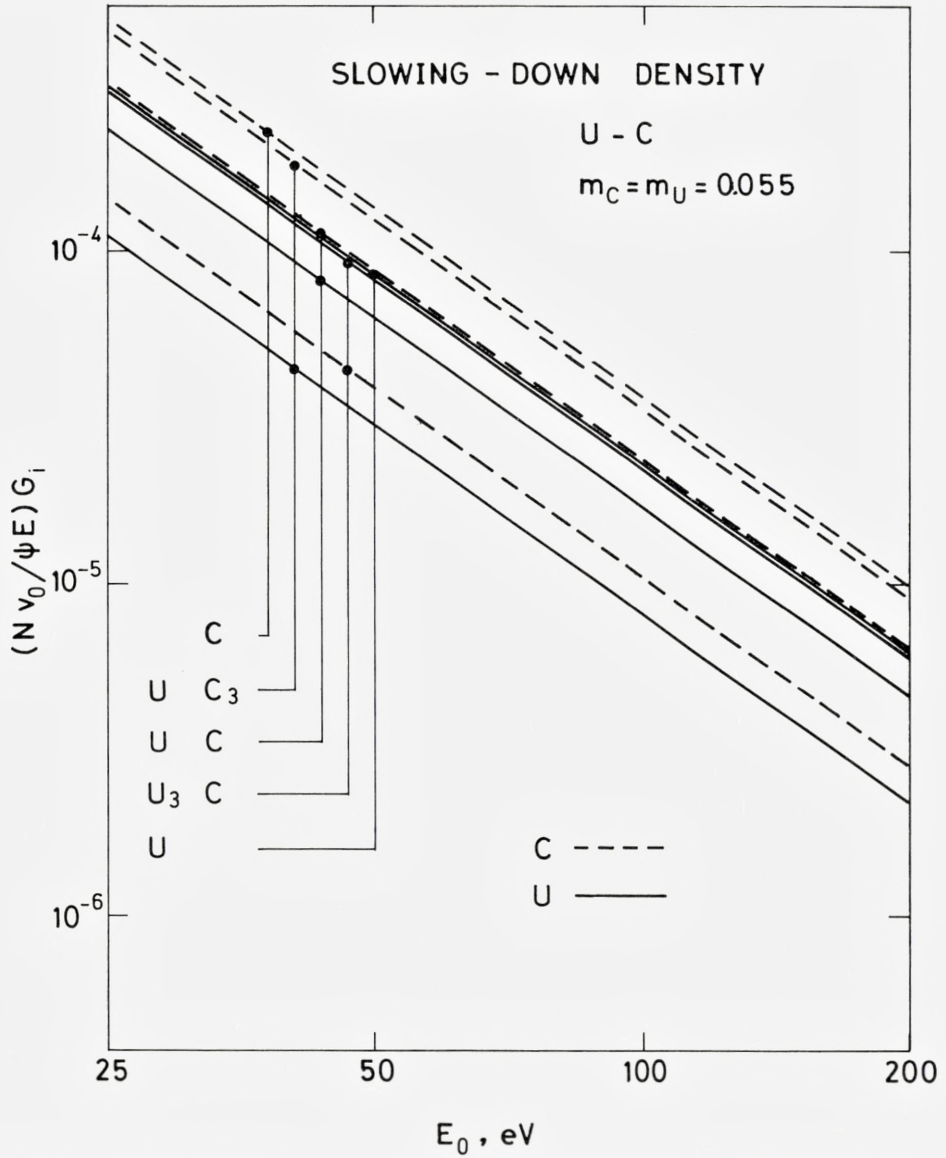

Fig. 1d. Uranium carbide, $m_C = m_U$; this graph is presumably less realistic than fig. 1c.

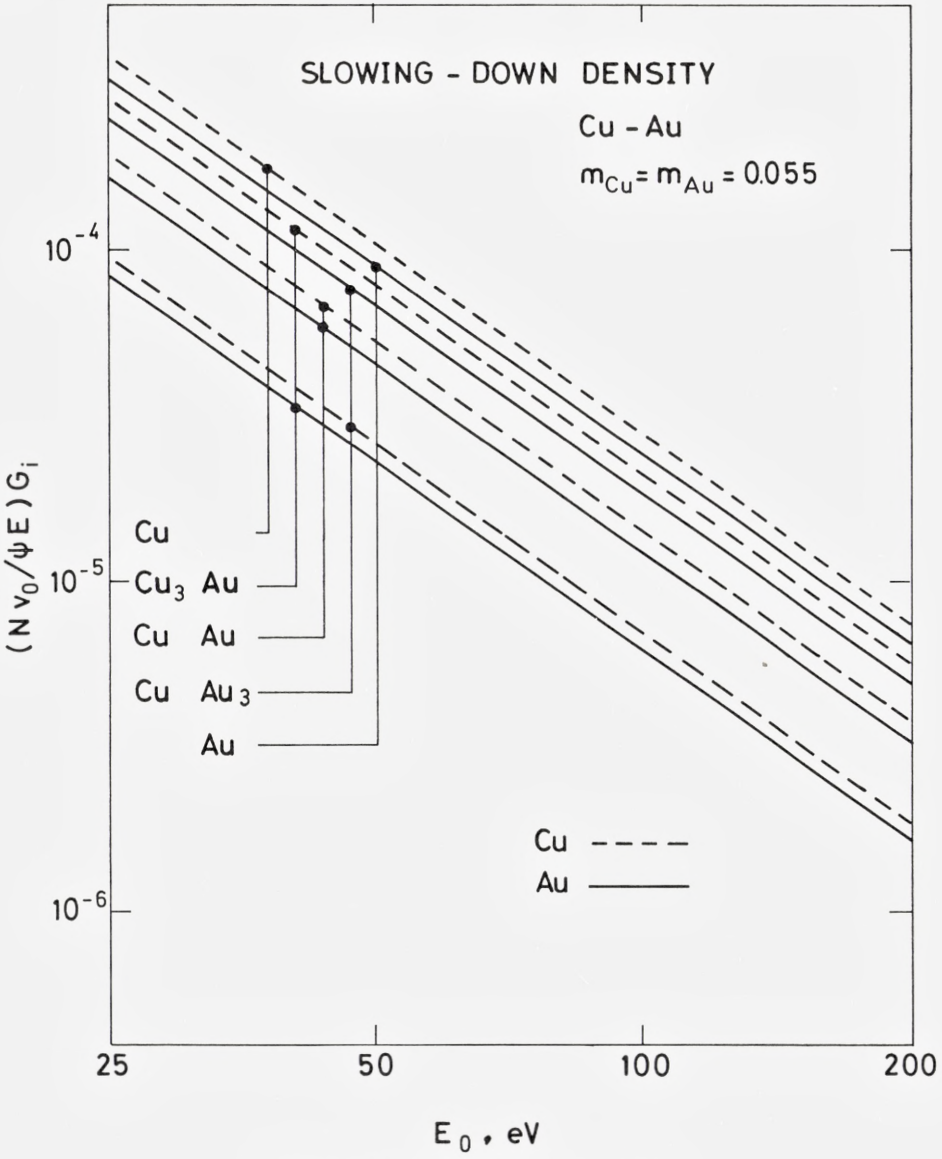

Fig. 1e. Copper-gold alloy, $m_{Cu} = m_{Au}$.

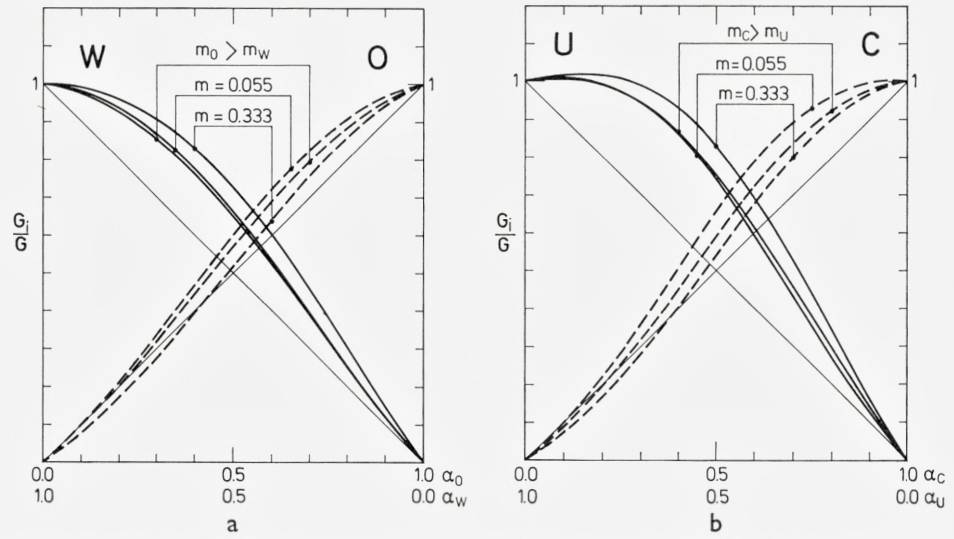

Fig. 2. Slowing-down densities G_1 and G_2 of each of the two constituents of three binary compounds, normalized to the values of the respective pure media, G, as a function of concentration. The ratios G_i/G do not depend on spectral energy E_0. In addition to the two combinations of scattering parameters m_i used in fig. 1, a third one with $m_1 = m_2 = 0.333$ has been included for illustration. Full-drawn and stipled lines refer to the heavy and light constituent, respectively. Apart from a constant factor given by eq. (25a) or 25b), thin fulldrawn lines refer to stoichiometric variation.

Fig. 2a. Tungsten oxide. The two curves with $m_O > m_W$ are presumed to come closest to reality.
Fig. 2b. Uranium carbide. The two curves with $m_C > m_U$ are presumed to come closest to reality.

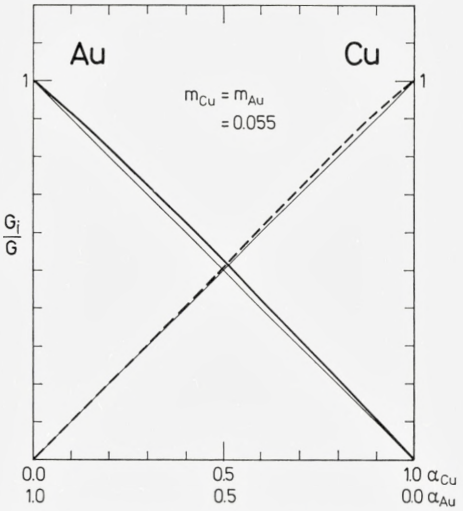

Fig. 2c. Copper-gold alloy. Only the two curves with $m_{Cu} = m_{Au}$ have been included.

case of $m_O > m_W$ and $m_O = m_W$, respectively. The variation of the expression (35) at fixed energy with composition is illustrated in fig. 2a. We notice that the variation of G_i near $\alpha_i = 1$ is much weaker than the stoichiometric variation. The qualitative conclusion appears justified that the total number of moving matrix atoms in a nearly pure target is almost unaffected by alloying impurities of widely different mass.

This effect can be understood qualitatively. The slowing-down density is determined both by the number of atoms set in motion and the time for slowing-down. Alloying an impurity of very different mass causes a decrease in the former quantity (the recoil density), but an increase in the latter.

As might be expected, this effect is even more pronounced in the case of *U-C* (figs. 1c + d and 2b), and less pronounced in *Cu-Au* (figs. 1e and 2c).

The recoil density, F_i, is determined by eqs. (27a, b),

$$\frac{1}{E} \cdot F_i = E_0^{-2} \cdot C_i; \quad E_0 \ll E, \tag{36}$$

where $C_i = \alpha_i \cdot K_i$. The variation of the expression (36) with recoil energy E_0 for W and O in W–O compounds is shown in figs. 3a + b for $m_O > m_W$ and $m_O = m_W$, for concentration 0, 1/4, 1/2, 3/4 and 1. For $m_O > m_W$, the *heavier* component recoils preferentially. This arises from the sensitivity of the recoil density to the steepness of the differential cross section[2, 33], the latter being greatest for the largest value of m according to eq. (9).

The variation of the displacement efficiency K_i with concentration is shown in fig. 4a. As one might expect, the displacement efficiency is almost independent of concentration in the vicinity of $\alpha_i = 1$. When α_i becomes smaller, K_i drops gradually to a significantly lower value. The relatively low displacement efficiency of impurities ($\alpha \ll 1$) is due to the comparatively inefficient energy transfer in collisions with host atoms and the small chance for impurity-impurity collisions. The same features are observed for *U-C* and *Cu-Au*, see figs. 3c–e and 4b + c.

Figs. 5a–c contain the same information as fig. 4. We have plotted the factor Y in eq. (28a) as a function of concentration. This factor represents the (concentration-dependent) deviation from stoichiometric behaviour of the recoil density. The upper and lower limits of Y are determined by eqs. (28b, c).

To make sure that our results do not hinge heavily on the detailed assumptions concerning the displacement process, we estimated in appendix B the influence of an atomic binding energy, and especially the significance of different binding energies of the two constituents, on the slowing-down density.

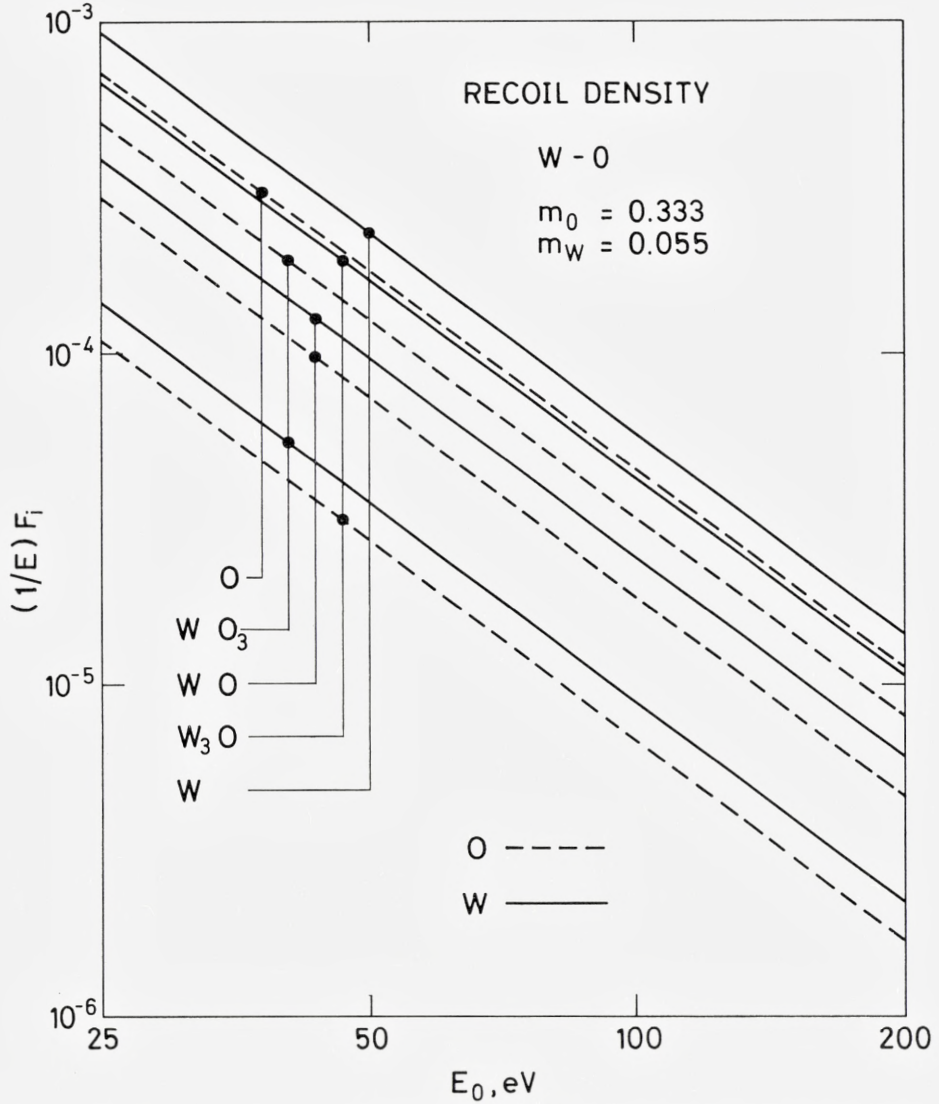

Fig. 3. Same as fig. 1 for the recoil densities, eq. (36). Note that all energy dependence goes as E_0^{-2}.

Fig. 3a. Tungsten oxide, $m_O > m_W$.

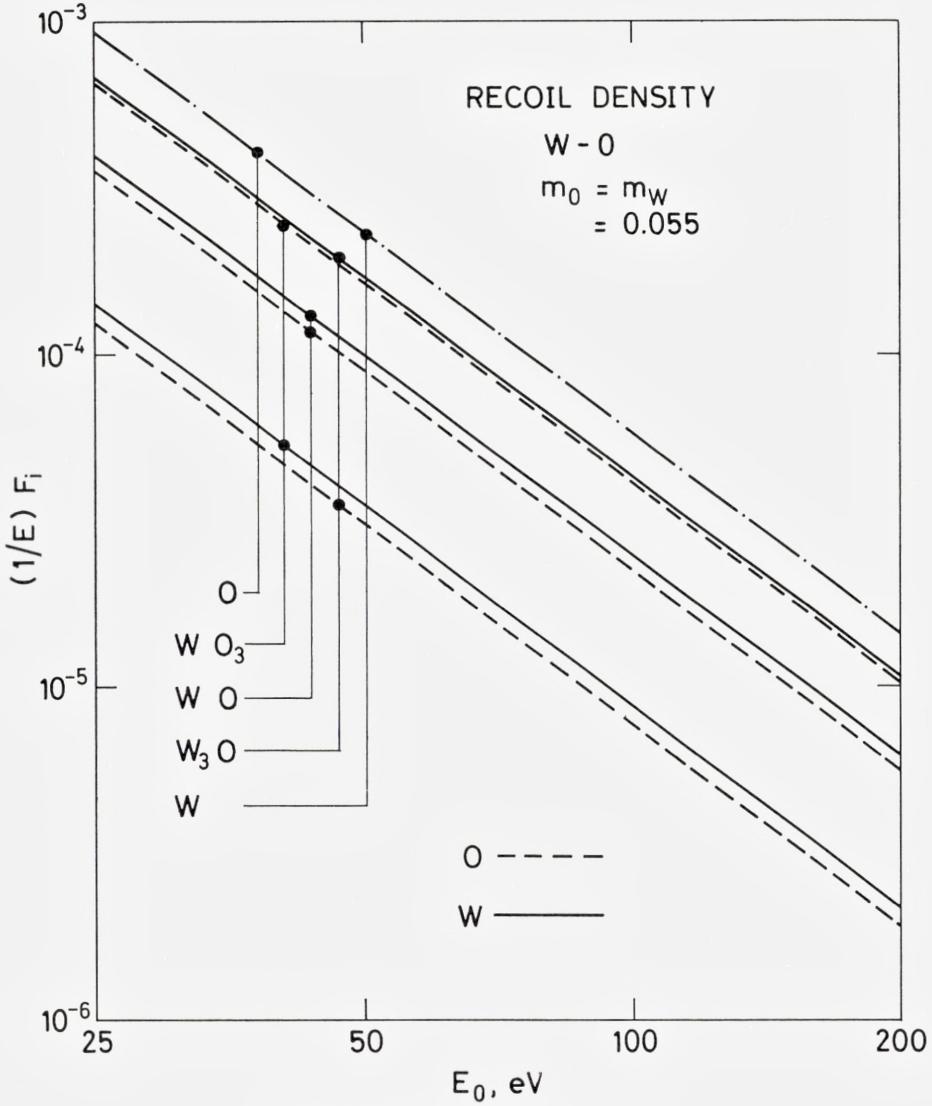

Fig. 3b. Tungsten oxide, $m_O = m_W$.

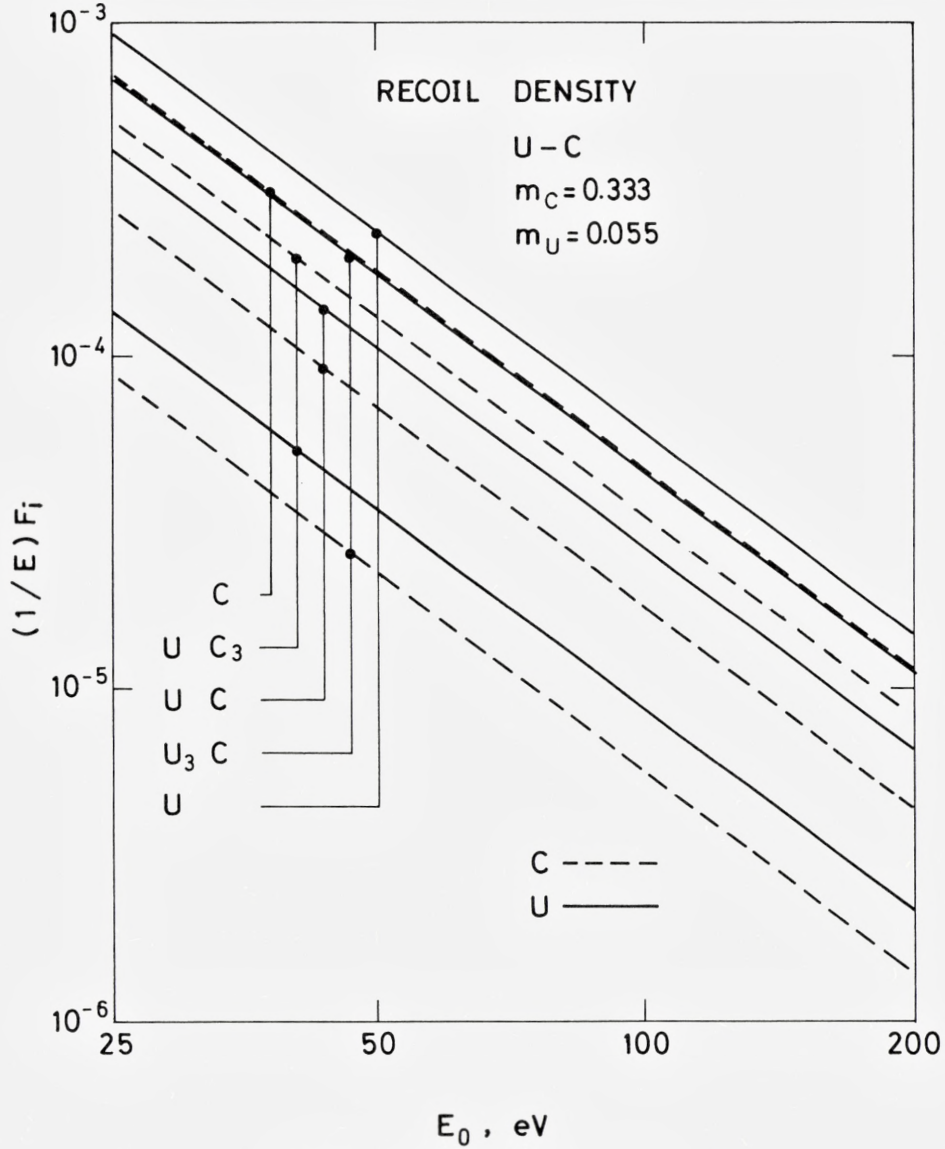

Fig. 3c. Uranium carbide, $m_C > m_U$.

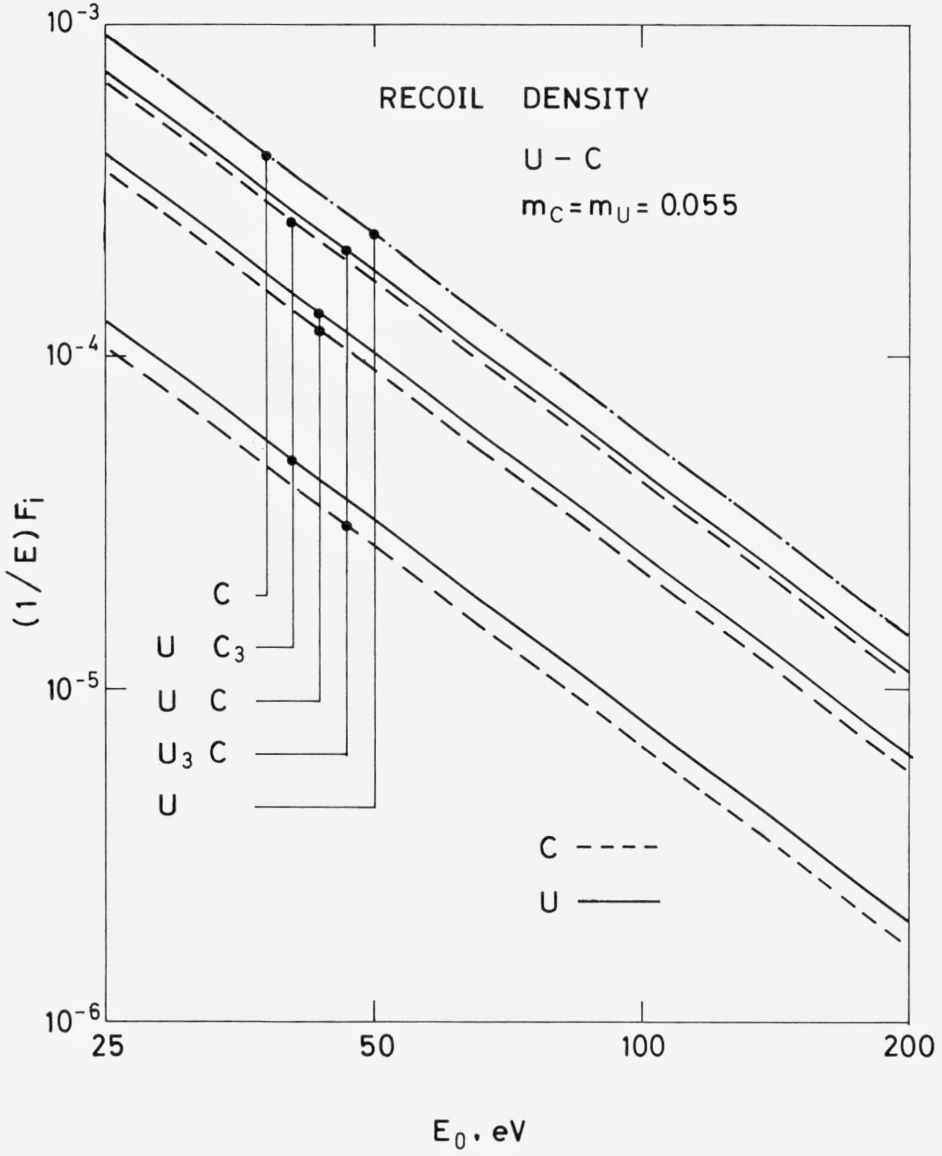

Fig. 3d. Uranium carbide, $m_C = m_U$.

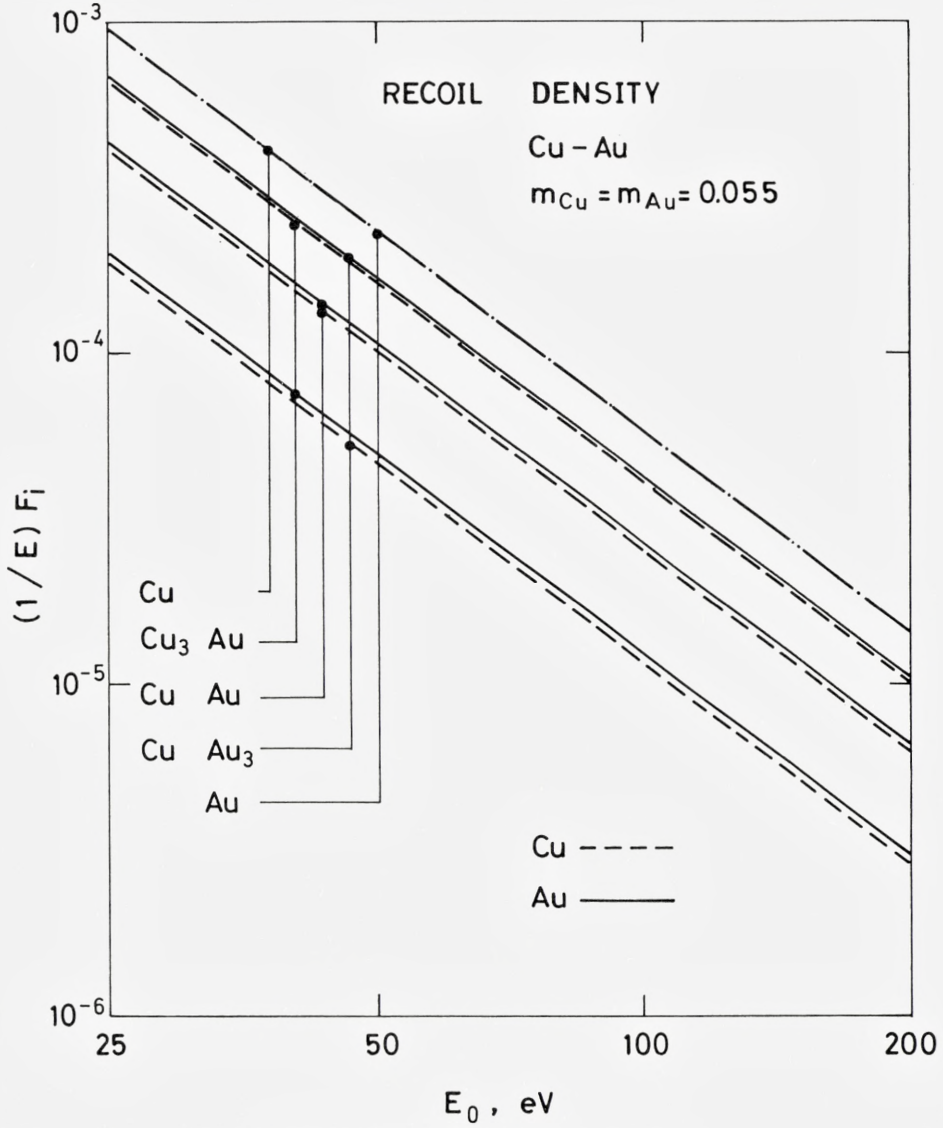

Fig. 3e. Copper-gold alloy, $m_{Cu} = m_{Au}$.

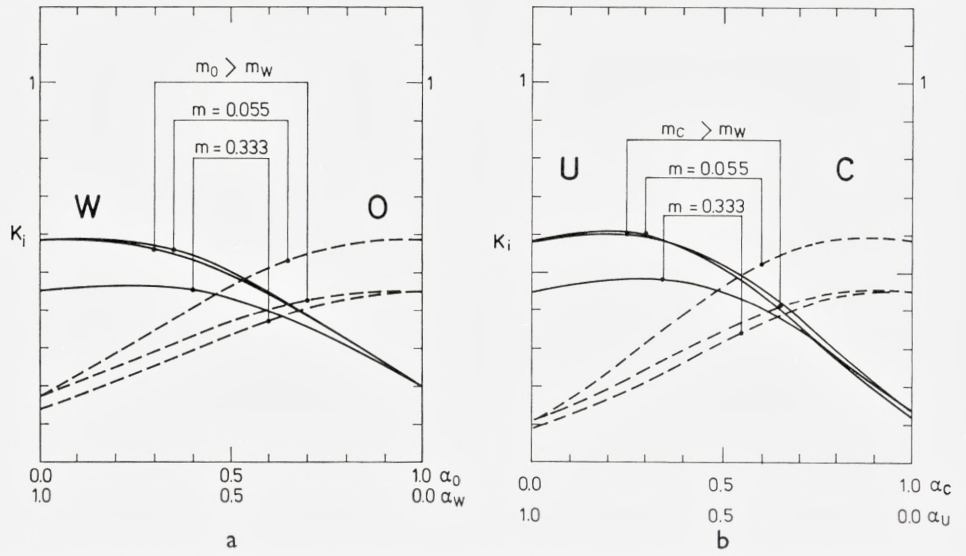

Fig. 4. Displacement efficiencies K_1 and K_2, eq. (33), of the two constituents of three binary compounds, as a function of concentration. As in fig. 2, three combinations of scattering parameters m_1 and m_2 were used. Full-drawn and stipled lines refer to the heavy and light constituent, respectively. Stoichiometric behaviour would correspond to straight horizontal lines.

Fig. 4a. Tungsten oxide. The two curves with $m_O > m_W$ are presumed to come closest to reality.
Fig. 4b. Uranium carbide. The two curves with $m_O > m_W$ are presumed to come closest to reality.

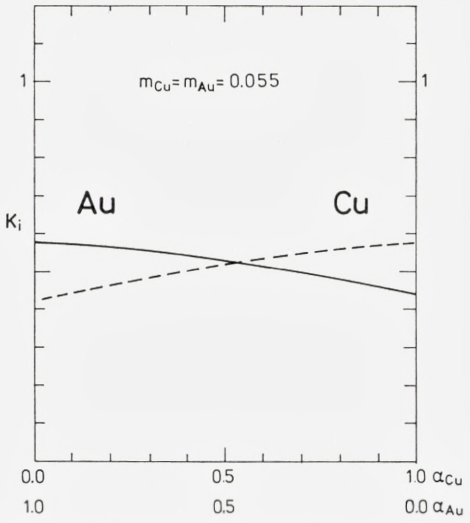

Fig. 4c. Copper-gold alloy. Only the two curves with $m_{Cu} = m_{Au}$ have been included.

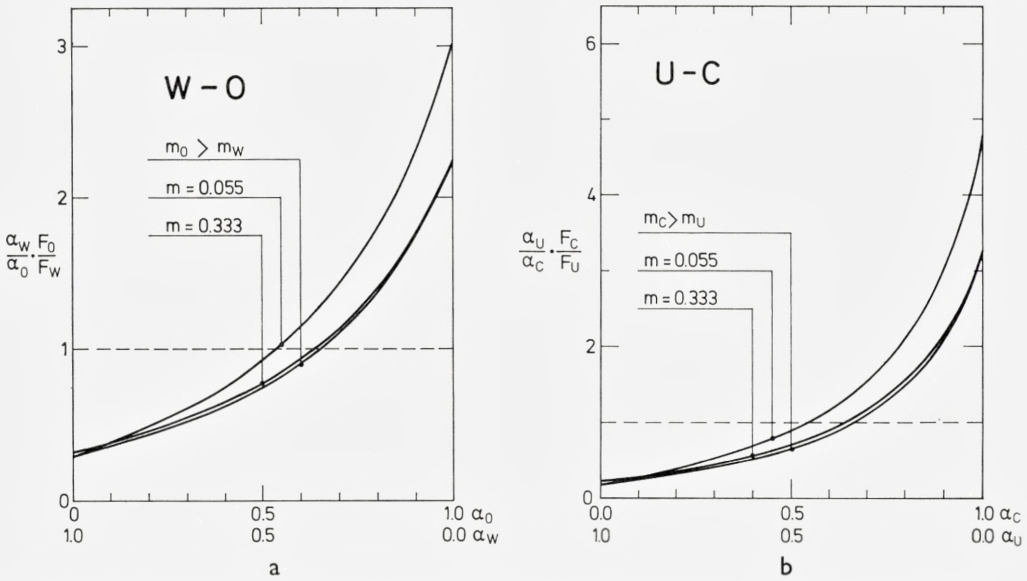

Fig. 5. Ratio of recoil densities of the constituents in three binary compounds, normalized so that stoichiometric behaviour would correspond to the dashed horizontal line. As in fig. 2, three combinations of scattering parameters m_1 and m_2 were used. Note the different scale in fig. 5b.

Fig. 5a. Tungsten oxide.
Fig. 5b. Uranium carbide.

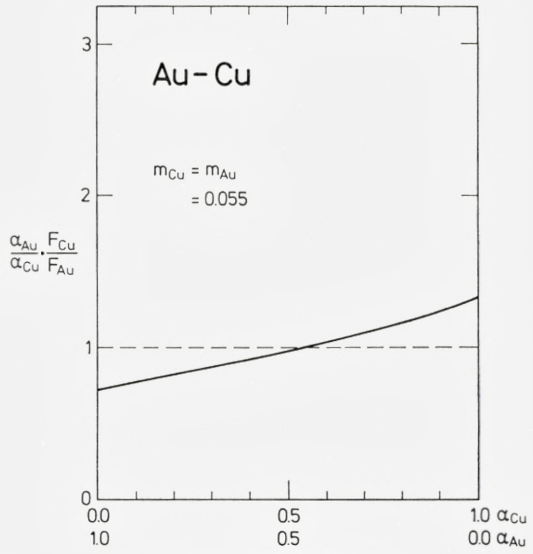

Fig. 5c. Copper-gold alloy.

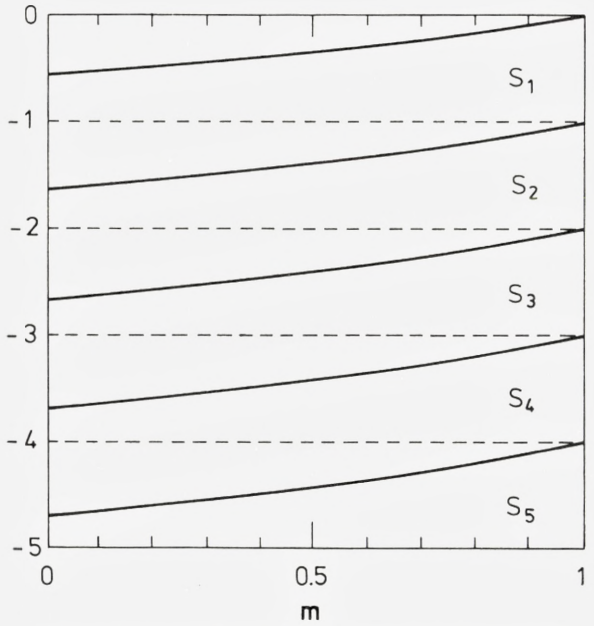

Fig. 6. The poles s_i of the Laplace transform $\tilde{G}(s)$ for a monatomic medium, as a function of m. The principal pole at $s^{(0)} = 1$ has been omitted.

7. Range of Validity of the Asymptotic Solutions

We should like to estimate the range of validity of the asymptotic solutions (24) and (27). This is conveniently done by finding the correction terms in the asymptotic expansions, i.e. determining residues at subsequent poles of the Laplace Transforms, $\tilde{G}_{ij}(s)$ and $\tilde{F}_{ij}(s)$.

In the case of a monatomic target, this problem has been discussed in ref. 34, in which it is shown that the higher-order poles, $s^{(1)}, s^{(2)}, \ldots$, etc. obey the inequalities $-i + m < s^{(i)} < -i + 1$. The positions of the poles $s^{(1)}, \ldots, s^{(5)}$, in the monatomic case, for $0 < m < 1$, are plotted in fig. 6. No poles are found in the interval $0 \leq s < 1$. Therefore, for a monatomic target the asymptotic solution has a remarkably large range of validity[1)].

In the binary or polyatomic case, the situation is substantially more complicated because eq. (6) only holds for the principal term in the asymptotic expansion. The subsequent terms do not only depend on the target (j) but also explicitly on the projectile (i). For the sake of simplicity we restrict the discussion to binary targets and analyse the possibility of poles ocurring

between zero and $s = 1$. However, since eq. (6) is not generally valid we want to treat the problem for an arbitrary projectile, 3. This is conveniently done by considering a ternary target (sect. 5) with species 1, 2, 3, but $\alpha_3 = 0$. The complete set of solutions of eq. (12) is then given by :

$$\left.\begin{aligned}
\tilde{G}_{13} &= 0 \\
\tilde{G}_{23} &= 0 \\
\tilde{G}_{33} &= B_3/[\beta_{31}\varepsilon_{31} + \beta_{32}\varepsilon_{32}] \\
\tilde{G}_{12} &= B_2 \cdot \beta_{12}/D^{(2)} \\
\tilde{G}_{22} &= B_2 \cdot \{\beta_{11}(\varepsilon_{11}-1) + \beta_{12}\varepsilon_{12}\}/D^{(2)} \\
G_{32} &= B_2 \cdot \{\beta_{12}\beta_{31} + \beta_{32}[\beta_{11}(\varepsilon_{11}-1) + \beta_{12}\varepsilon_{12}]\}/\{D^{(2)}[\beta_{31}\varepsilon_{31} + \beta_{32}\varepsilon_{32}]\} \\
\tilde{G}_{11} &= B_1 \cdot \{\beta_{22}(\varepsilon_{22}-1) + \beta_{21}\varepsilon_{21}\}/D^{(2)} \\
\tilde{G}_{21} &= B_1 \cdot \beta_{21}/D^{(2)} \\
\tilde{G}_{31} &= B_1 \cdot \{\beta_{21}\beta_{32} + \beta_{31}[\beta_{22}(\varepsilon_{22}-1) + \beta_{21}\varepsilon_{21}]\}/\{D^{(2)}[\beta_{32}\varepsilon_{32} + \beta_{31}\varepsilon_{31}]\}
\end{aligned}\right\} \quad (37)$$

where we have used the notation of sect. 4. Of these equations, only the six lower ones are of interest here. Furthermore, because of symmetry we may concentrate on the lower three equations. The poles and residues of $\tilde{G}_{11}$, $\tilde{G}_{21}$ and $\tilde{G}_{31}$ determine the number of moving 1-atoms when particles of type 1, 2, or 3 impinge on a 1–2 compound. Writing $\tilde{G}_{31}$ in the form

$$\tilde{G}_{31} = \frac{\beta_{32}}{\beta_{32}\varepsilon_{32} + \beta_{31}\varepsilon_{31}}\tilde{G}_{21} + \frac{\beta_{31}}{\beta_{32}\varepsilon_{32} + \beta_{31}\varepsilon_{31}}\tilde{G}_{11} \quad (38)$$

facilitates the discussion.

From eq. (13a) it follows that $|\beta_{ik}| = \infty$ for $s = m_k$; otherwise β_{ik} is finite and nonzero. According to (13b), the product $\beta_{ik}\varepsilon_{ik}$ is zero for $s = 0$, positive for $s > 0$ and negative for $s < 0$. Therefore, poles of $\tilde{G}_{31}$ may only occur at

(i) $s = 0$,
(ii) $s = m_1$ or m_2, and
(iii) the poles of $\tilde{G}_{11}$ and $\tilde{G}_{21}$.

For $s = 0$, insertion of eqs. (13a) and (13b) into (37) shows that $\tilde{G}_{11}$ and $\tilde{G}_{21}$ have finite values at this point; $\tilde{G}_{31}$ has a pole at zero because of the vanishing factor $\beta_{32}\varepsilon_{32} + \beta_{31}\varepsilon_{31}$ in the denominator.

The occurrence of poles at $s = m_1$ or m_2 depends on whether or not some (or all) of the parameters m_1, m_2, and m_3 are identical. It can happen that $\tilde{G}_{31}$ has a pole here, but not $\tilde{G}_{11}$ or $\tilde{G}_{21}$.

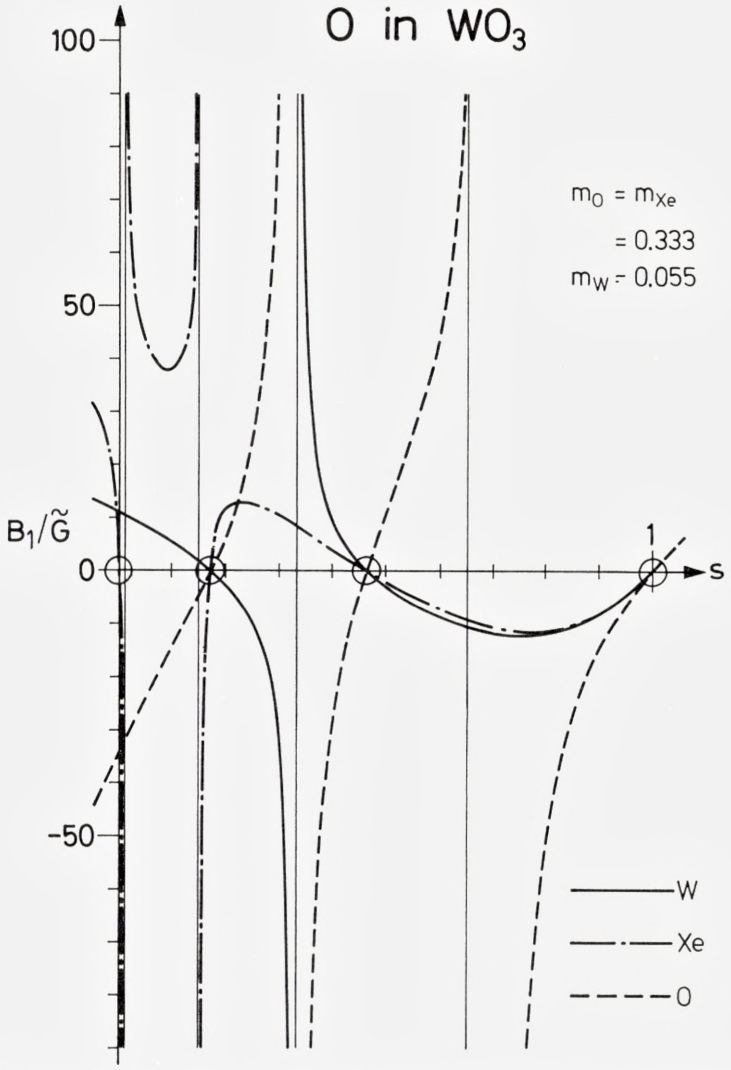

Fig. 7. Deviation of the slowing-down density $G_{ij}(E,E_0)$ from asymptotic behaviour. We plot reciprocal Laplace transforms $\tilde{G}_{11}$, $\tilde{G}_{21}$, and $\tilde{G}_{31}$ versus s. For details see text.

Fig. 7a. Moving oxygen atoms in WO_3

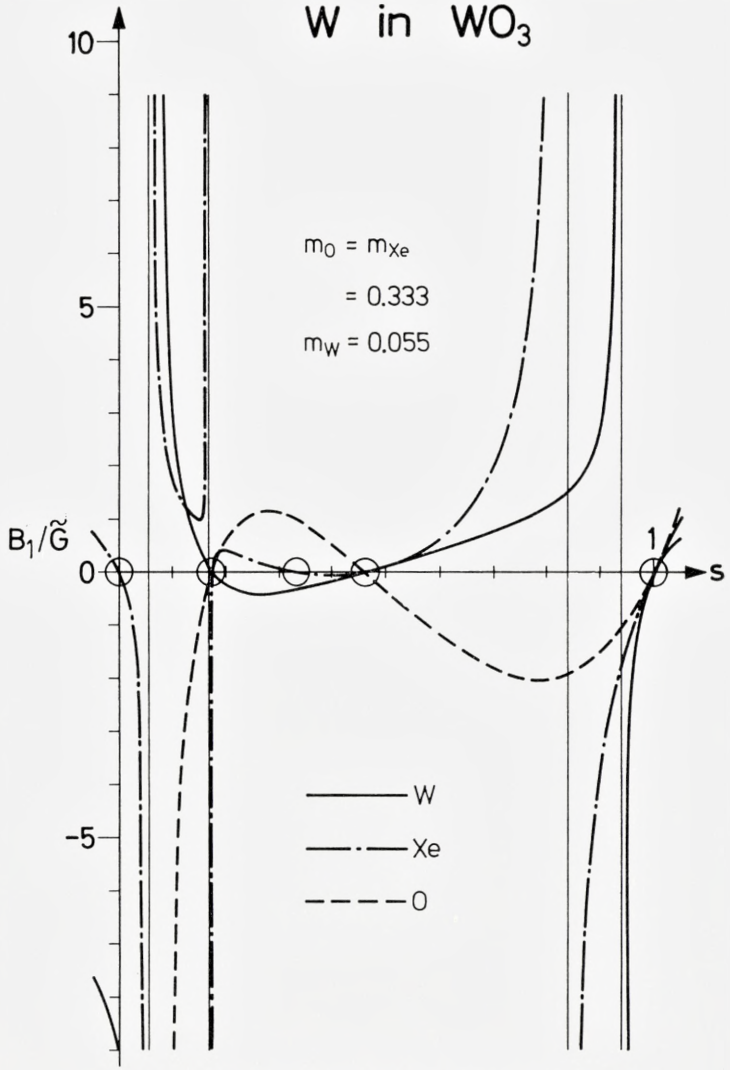

Fig. 7b. Moving tungsten atoms in WO_3.

The number and distribution of poles in the remaining part of the interval will depend on the parameters α_i, C_{ik}, and m_i.

We have analysed numerically the case of a *W-O* compound bombarded with *W*, *O* and *Xe*. The positions and residues of the poles of $\tilde{G}_{11}$, $\tilde{G}_{21}$ and $\tilde{G}_{31}$ were determined, and their variation with concentration and choice of scattering parameters was investigated. Since the parameters are chosen so as to give a good description at low spectral energies, i.e. near $s = 1$, caution is required in drawing detailed physical conclusions from the correction terms to asymptotic behaviour.

An example is given in fig. 7a and b. For clarity, we have plotted the *reciprocal* values of $\tilde{G}_{11}$, $\tilde{G}_{21}$ and $\tilde{G}_{31}$ versus s, so that the poles of the $\tilde{G}$-functions show up as zeros, and the residues may be determined from the inverse *slope* of the $1/\tilde{G}$ – curve.

Fig. 7a shows the $1/\tilde{G}$ – functions for oxygen in a WO_3 target bombarded with oxygen, tungsten, or xenon, corresponding to $\tilde{G}_{11}$, $\tilde{G}_{21}$ or $\tilde{G}_{31}$, respectively. We first note that all three curves pass through $s = 1$ with identical slopes, as it should be expected from the results of sect. 3. Second, we notice that $1/\tilde{G}_{31}$ has the expected zero at $s = 0$, and the other two curves do not.

Two additional zeros occur at $s_2 \sim 0.17$ and $s_1 \sim 0.46$; these are common for all three curves. Thus, the second term in the asymptotic expansion varies approximately as $\sqrt{E/E_0}$ in all three cases. As may be seen from the figure, the residues at the second pole s_1 are comparable in magnitude to the residuum at $s = 1$.

Fig. 7b shows the corresponding curves for tungsten in WO_3, bombarded with tungsten ($\tilde{G}_{11}$), oxygen ($\tilde{G}_{21}$) or xenon ($\tilde{G}_{31}$). A very similar behaviour is observed, except that an additional zero occurs at $s = 0.333$ for $1/\tilde{G}_{31}$. Again, we observe that the second term in the expansion varies approximately as $\sqrt{E/E_0}$.

We conclude that the occurence of poles in the interval between zero and one narrows the range of validity of the asymptotic solution as compared to the monatomic case. As a rule-of-thumb the second term varies approximately as $\sqrt{E/E_0}$ as a function of energy.

8. Discussion

The major uncertain quantity entering the theory is the constant C in the power cross section (9), in particular its value and mass dependence for $m < 1/4$, eq. (10b). Therefore, the results presented in fig. 1 for the slowing-down density can at most be considered qualitative. The other graphs, in particular figs. 2 and 4, show the slowing-down and recoil densities in a suitably normalized form so that the inherent error is minimized.

Consider the recoil density first, and its connection with the number of displaced atoms. Previous work in this field[21-23] concentrated on the *total* number of displacements created in a compound target by a primary particle. The displacement model of KINCHIN & PEASE[36] was usually adopted as well as a strongly simplified model for the scattering cross sections. BARODY[21] in particular assumed a fixed concentration, $\alpha_1 = \alpha_2 = \frac{1}{2}$. The main uncertainty was the displacement model which, for a binary target, contains at least four, perhaps six, essentially unknown parameters, i.e. two displacement thresholds, two replacement energies and, perhaps, two lattice binding energies. In most applications, the displacement and replacement energies were all set equal ($''=E_d''$), and the binding energies were either ignored or set equal E_d, too.

In the present calculations, we allowed for more realistic scattering cross sections, in particular for different energy dependences of the various cross sections involved. Except for appendix B we ignored binding energies, but eliminate a substantial part of the remaining uncertainty by plotting individual displacement efficiencies rather than defect numbers.

Fig. 4b shows that, for a uranium target with a few per cent alloyed carbon, the displacement efficiency of uranium atoms is six times as great as that of carbon atoms. In addition, when the carbon content increases from 0 to 40 per cent, the displacement efficiency for uranium remains essentially unchanged while the one for carbon increases by a factor of three, approximately linear with concentration. To our knowledge, such pronounced deviations from stoichiometric behaviour have not been predicted previously.

We are not aware of any experimental results that could be analysed directly in terms of a graph like fig. 4. Experiments to check these predictions (e.g. by channeling[37]) seem most promising when dealing with low, but varying concentration of one of the two species, since then the displacement threshold energies may be considered with reasonable confidence to be independent of concentration.

Obviously, fig. 4 predicts a pronounced difference in the behaviour of *dopant atoms* under irradiation between the case of bombarding electrons (where single defects dominate) and bombarding heavy ions or fast neutrons (where displacement cascades dominate).

Let us now go over to sputtering. According to ref. 28, the flux of sputtered atoms is determined by

i) the slowing-down density,
ii) the spatial distribution of deposited energy,
iii) the surface binding energy.

The two key problems in the sputtering of compound targets are

a) how is the total sputtering yield related to the sputtering yields of the respective pure targets, and
b) what is the composition of the sputtered material.

We have to note that any deviation from stoichiometric sputtering will cause a change in composition of the remaining target material, such that the target is no longer homogeneous. Homogeneity, however, is a vital assumption entering our basic equations. Thus, the present theory can at most be applied to low-dose sputtering experiments, i.e., experiments involving sputtering of, say, one monolayer of target atoms. Such experiments have been performed on pure metallic targets (e.g. ANDERSEN & BAY[13]) but, with one exception (see below) not on compound targets. The following considerations will, therefore, be kept brief and qualitative.

It is appropriate to distinguish between sputtering experiments performed at low and high bombarding energy, the former category referring to energies around or below 1 keV. Pronounced depletion of surface layers due to preferential sputtering has been reported in low-energy sputtering experiments (e.g. ASADA et al.[4]), ANDERSON[7]), TARNG et al. [9]). Because of the small penetration depth of low-energy ions, only a very shallow surface layer can be involved in the sputtering process proper. The occurrence of a massive depleted layer is, therefore, indicative of a competing migrational process. Such a process may also be a disturbing factor in high-energy sputtering experiments, and its influence needs to be checked by, e.g., variation of the target temperature during bombardment.

A number of higher-energy sputtering experiments dealt with the Cu_3Au system[4–6, 8]). In high-dose experiments a gold-rich surface layer was observed[5, 6]). However, quantitative data on sputtering yields were only determined by OGAR et al.[8]). No bombardment doses were given, but since the sputtered

material was detected by neutron activation, one may assume that only few atomic layers were removed. The copper:gold sputtering ratio for Ar^+ and Hg^+ bombardment in the 10 keV region was observed to be slightly smaller than 3:1. The authors proposed preferred migration of gold atoms to the surface as an explanation. Since the observed deviation from stoichiometry is rather small ($\lesssim 10\ \%$) it does not appear feasible to make a definite statement on the actual source of nonstoichiometry. The slowing-down densities excluding bulk binding forces behave in such a way that preferential motion of copper atoms would be predicted (eq. 25b). However, inclusion of binding forces produces a shift in the right direction, the magnitude being uncertain (appendix B). Inclusion of, e.g., focused collision sequences in the sputtering mechanism would seem to enhance the contribution of copper atoms rather than decrease it. Finally, if gold atoms should migrate indeed preferentially, one might also have to consider the possibility of a lower surface binding energy of gold atoms.

Ogar et al. also determined absolute partial sputtering yields for copper and gold atoms, respectively. They report a partial sputtering yield for copper from the Cu_3Au alloy that is about twice as large as the sputtering yield of pure copper under equivalent bombardment conditions. It follows from fig. 2c that such a pronounced effect cannot originate in a drastic change of the slowing-down density as compared to the pure target. Neither does it appear feasible that the surface binding energy of copper atoms differs by a factor of two from the one valid for a pure copper target. We assert the change in sputtering yield to be essentially due to the different spatial distribution of deposited energy. Indeed, alloying heavy gold atoms to a copper target causes a pronounced decrease in ion penetration due to increased importance of large-angle scattering[1, 20] and, therefore, increased energy deposition at the target surface. A quantitative evaluation is not given here since the measurements of Ogar et al. were done on Cu_3Au single crystals while existing calculations refer to random targets.

Pronounced deviations are expected from stoichiometric sputtering in metallic alloys of very different masses. Figs. 2a and 2b indicate that the fluxes of both the heavy and the light constituent *increase* as compared to the pure targets, in terms of the respective concentrations. The flux of *heavy* atoms increases most pronouncedly. However, the ratio of fluxes at any given concentration behaves in a more complicated manner. Figs. 1a and 1c show that there may be different energy dependences, and comparing, e.g., figs. 1a and 1b, one may notice that preferential sputtering of the heavy constituent may be predicted from fig. 1a, and the light one from fig. 1b. In case

of WO_3, our preference of the choice of potential constants is such as to predict preferential sputtering of W. This preference is, however, not so strong as the corresponding one with the uranium carbide system.

Systematic investigations of the sputtering of oxides[10] revealed preferential sputtering of oxygen in many cases. Consistently, oxygen happened to be the lighter constituent. The analysis indicated a contribution of chemical and local-heating effects. From the point of view of the present investigation, it would be of considerable interest to have similar experimental results taken at low bombardment doses.

Acknowledgements

We should like to thank H. H. Andersen, R. Behrisch, and J.W. Mayer for clarifying discussions, and H. Dreyer Nielsen and his crew for careful preparation of the drawings.

Appendix A

We want to show that the determinant of the system of equations (12) has no zero for $s > 1$. First, it follows from eqs. (13) and (14) that $\beta_{ik} > 0$ and $\varepsilon_{ik} > 1$ for $s > 1$.

Now, let $\beta = (\beta_{ik})$ be an arbitrary $n \times n$ matrix with positive elements, $\beta_{ik} > 0$, and let ε_{ik}, where $i, k = 1, \ldots, n$ be a set of n^2 arbitrary elements. We define another $n \times n$ matrix $\Delta = (\Delta_{ik})$ by

$$\Delta_{ik} = \delta_{ik} \cdot \sum_j \beta_{ij} \varepsilon_{ij}$$

and will now prove the following theorem for the determinant

$$det\,(\Delta - \beta) =$$

$$= \begin{vmatrix} \beta_{11}(\varepsilon_{11} - 1) + \beta_{12}\varepsilon_{12} + \ldots + \beta_{1n}\varepsilon_{1n} & \ldots & -\beta_{1n} \\ -\beta_{21} & \beta_{22}(\varepsilon_{22} - 1) + \beta_{21}\varepsilon_{21} + \ldots + \beta_{2n}\varepsilon_{2n} \quad \ldots & -\beta_{2n} \\ \cdot & \cdot \quad \cdot & \cdot \\ \cdot & \cdot \quad \cdot & \cdot \\ \cdot & \cdot \quad \cdot & \cdot \\ -\beta_{n1} & -\beta_{n2} \ldots \beta_{nn}(\varepsilon_{nn} - 1 + \beta_{n1}\varepsilon_{n1} + \ldots + \beta_{n\,n-1}\varepsilon_{n\,n-1} \end{vmatrix}$$

If all elements $\varepsilon_{ik} > 1$ *then* $det\,(\Delta - \beta) > 0$.

The theorem is proved by induction, increasing the dimension of the matrix from n–1 to n.

i) The case $n = 1$ is trivial: $det(\Delta - \beta) = \beta_{11}(\varepsilon_{11} - 1)$

Since $\beta_{11} > 0$ and $\varepsilon_{11} > 1$, $det(\Delta - \beta) > 0$.

ii) The general step $n - 1 \to n$: We first note that if all $\varepsilon_{ik} = 1$ then $det(\Delta - \beta) = 0$, because the sum of the elements in each row is zero. It is, therefore, sufficient to show that for $\varepsilon_{ik} > 1$, $det(\Delta - \beta)$ is a strictly increasing function of all the ε_{ik}, or:

$$\frac{\partial}{\partial \varepsilon_{ik}} det(\Delta - \beta) > 0 \quad \text{for all} \quad \varepsilon_{i'k'} > 1.$$

For reasons of symmetry it is sufficient to consider the case $i = 1$. We get by differentation:

$$\frac{\partial}{\partial \varepsilon_{1k}} \begin{vmatrix} \beta_{11}(\varepsilon_{11} - 1) + \beta_{12}\varepsilon_{12} + \ldots + \beta_{1n}\varepsilon_{1n} & -\beta_{12} & \ldots & -\beta_{1n} \\ -\beta_{21} & \beta_{22}(\varepsilon_{22} - 1) + \beta_{21}\varepsilon_{21} + \ldots + \beta_{2n}\varepsilon_{2n} & \ldots & -\beta_{2n} \\ \cdot & \cdot \quad \cdot & & \cdot \\ \cdot & \cdot & & \cdot \\ \cdot & \cdot & & \cdot \\ -\beta_{n1} & -\beta_{n2} & \beta_{nn}(\varepsilon_{nn} - 1) + \beta_{n1}\varepsilon_{n1} + \ldots + \beta_{nn-1}\varepsilon_{nn-1} & \end{vmatrix}$$

$$= \begin{vmatrix} \beta_{1k} & -\beta_{12} & \ldots & -\beta_{1n} \\ 0 & \beta_{22}(\varepsilon_{22} - 1) + \beta_{21}\varepsilon_{21} + \ldots + \beta_{2n}\varepsilon_{2n} & \ldots & -\beta_{2n} \\ \cdot & \cdot \quad \cdot & & \cdot \\ \cdot & \cdot & & \cdot \\ \cdot & \cdot & & \cdot \\ 0 & -\beta_{n2} & \beta_{nn}(\varepsilon_{nn} - 1) + \beta_{n1}\varepsilon_{n1} + \ldots + \beta_{nn-1}\varepsilon_{nn-1} & \end{vmatrix}$$

$$= \beta_{1k} \begin{vmatrix} \beta_{22}(\varepsilon_{22} - 1) + \beta_{21}\varepsilon_{21} + \ldots + \beta_{2n}\varepsilon_{2n} & \ldots & -\beta_{2n} \\ \cdot & & \cdot \\ \cdot & & \cdot \\ \cdot & & \cdot \\ -\beta_{n2} & \ldots & \beta_{nn}(\varepsilon_{nn} - 1) + \beta_{n1}\varepsilon_{n1} + \ldots + \beta_{nn-1}\varepsilon_{nn-1} \end{vmatrix}$$

The last determinant is a $(n–1) \times (n–1)$ determinant, but in a form not suited for direct induction. However, the matrix can be brought into a suitable form by defining new quantities $\tilde{\varepsilon}_{ii}$ and $\tilde{\beta}_{ii}$ so that for $i = 2, \ldots, n$

1) $\beta_{ii}(\varepsilon_{ii} - 1) + \beta_{i_1}\varepsilon_{i_1} = \tilde{\beta}_{ii}(\tilde{\varepsilon}_{ii} - 1)$
2) $\tilde{\beta}_{ii} > 0$
3) $\tilde{\varepsilon}_{ii} > 1$

which is evidently possible. For $i \neq k$ we define $\tilde{\varepsilon}_{ik} = \varepsilon_{ik}$ and $\tilde{\beta}_{ik} = \beta_{ik}$. Then

$$\frac{\partial}{\partial\, \varepsilon_{1k}}\, det\, (\Delta - \beta) =$$

$$\beta_{1k} \begin{vmatrix} \tilde{\beta}_{22}(\tilde{\varepsilon}_{22}-1) + \tilde{\beta}_{23}\,\tilde{\varepsilon}_{23} + \ldots + \tilde{\beta}_{2n}\,\tilde{\varepsilon}_{2n} & \ldots & -\tilde{\beta}_{2n} \\ \cdot & \cdot & \cdot \\ \cdot & \cdot & \cdot \\ \cdot & \cdot & \cdot \\ -\tilde{\beta}_{n2} \ldots \tilde{\beta}_{nn}(\tilde{\varepsilon}_{nn} - 1) + \tilde{\beta}_{n2}\,\tilde{\varepsilon}_{n2} + & \ldots & +\tilde{\beta}_{nn-1}\,\tilde{\varepsilon}_{nn-1} \end{vmatrix}$$

Here $\beta_{1k} > 0$ and the determinant is positive too, since it is a $(n-1) \times (n-1)$-determinant of the type considered.

This proves the theorem.

Appendix B: Effect of Atomic Binding

We want to indicate briefly the effect of atomic binding on energy dissipation. Some results of similar calculations for monatomic targets have been reported previously[1, 27, 28], yet without derivation. A detailed discussion will be given in a forthcoming paper[35], but the main steps – for a polyatomic medium – will be sketched here.

We only consider the slowing-down density G_{ij}. If we assume that an atom of type i loses a binding energy V_i upon recoiling from its rest position, the only necessary change in eq. (2a) is replacement of the recoil term $G_{kj}(T, E_0)$ by

$$G_{kj}(T - V_k, E_0), \tag{B 1}$$

while the boundary condition (4) remains unchanged.

In the evaluation for power scattering, eq. (10), the Laplace transformation is carried out conveniently by means of expansion in powers of V_k/E_0. Then, the recoil term $\tilde{G}_{kj}(s)$ in eq. (12) is replaced by the expression

$$\sum_{\nu=0}^{\infty} \binom{-s-1}{\nu} (V_k/E_0)^{\nu}\, \tilde{G}_{kj}(s + \nu). \tag{B 2}$$

The resulting system of equations can be solved by perturbation expansion,

$$\tilde{G}_{kj}(s) = \sum_{\nu} \tilde{G}_{kj}^{(\nu)}(s), \tag{B 3}$$

where $\tilde{G}_{kj}^{(\nu)}(s)$ contains ν factors of the set $(V_1, V_2, \ldots)$. The zero-order term $\tilde{G}_{kj}^{(0)}(s)$ is identical with the one calculated in sect. 3, and the first-order term follows from the equations

$$\left.\begin{aligned} &\tilde{G}_{ij}^{(1)}(s) \sum_k \beta_{ik}(s)\, \varepsilon_{ik}(s) - \sum_k \beta_{ik}(s)\, \tilde{G}_{kj}^{(1)}(s) = \\ &= -(s+1) \sum_k (V_k/E_0)\, \beta_{ik}(s)\, \tilde{G}_{kj}^{(0)}(s+1). \end{aligned}\right\} \tag{B 4}$$

Only the inhomogeneity on the right-hand side differs from eq. (12). In particular, the highest poles of $\tilde{G}_{ij}^{(1)}(s)$ are determined by the zeros of the determinant $D(s)$, just as those of $\tilde{G}_{ij}^{(0)}(s)$. The asymptotic solution $G_{ij}^{(1)}(E, E_0)$ for $E \gg E_0$ is, therefore, proportional to E, and the same is true for all higher orders $G_{ij}^{(\nu)}(E, E_0)$. Note especially that the term on the right-hand side of (B4) is regular for $s > m_i$. Then, with the notations of sect. 4, the asymptotic solutions ($s = 1$) of (B 4) in the binary case can be written in the form

$$\left.\begin{aligned} &G_{11}^{(1)}/G_{11}^{(0)} \sim G_{21}^{(1)}/G_{21}^{(0)} \sim \\ &\sim -(2/D^{(2)}(2)) \{(\beta_{11}(1) + \beta_{12}(1))(V_1/E_0) \times \\ &[(\beta_{22}(2) - 1)\beta_{22}(2) + \beta_{21}(2)\beta_{21}(2)] + (\beta_{12}(1)/\beta_{21}(1)) \times \\ &(\beta_{21}(1) + \beta_{22}(1))\,(V_2/E_0)\,\beta_{21}(2)\}, \end{aligned}\right\} \tag{B 5}$$

where $D^{(2)}(s)$, $\varepsilon_{ik}(s)$, and $\beta_{ik}(s)$ are defined in eqs. (13a, b) and (22a).

In case of a monatomic medium (i.e. either for $M_1 = M_2$ and arbitrary α_1 or for $\alpha_1 = 1$ and arbitrary M_2/M_1), eq. (B5) reduces to the previously quoted result[27, 28]

$$G_{11}^{(1)}/G_{11}^{(0)} \sim -(2 - m_1)\, V_1/E_0 \qquad \text{for } M_1 = M_2 \tag{B 6}$$

as it should be.

We have evaluated eq. (B5) numerically for the tungsten-oxygen system. We write (B5) in the form

$$G_{11}^{(1)}/G_{11}^{(0)} \sim G_{21}^{(1)}/G_{21}^{(0)} \sim -R_1(V_1/E_0) - R_2(V_2/E_0) \tag{B 7}$$

and plot R_1 and R_2 in fig. 8a for oxygen and in fig. 8b for tungsten. It is seen that R_2 is vanishingly small in both cases. R_1 has its greatest value for the pure materials and drops off rapidly with increasing concentration of the alloyed impurity. This is particularly so in case of fig. 8b.

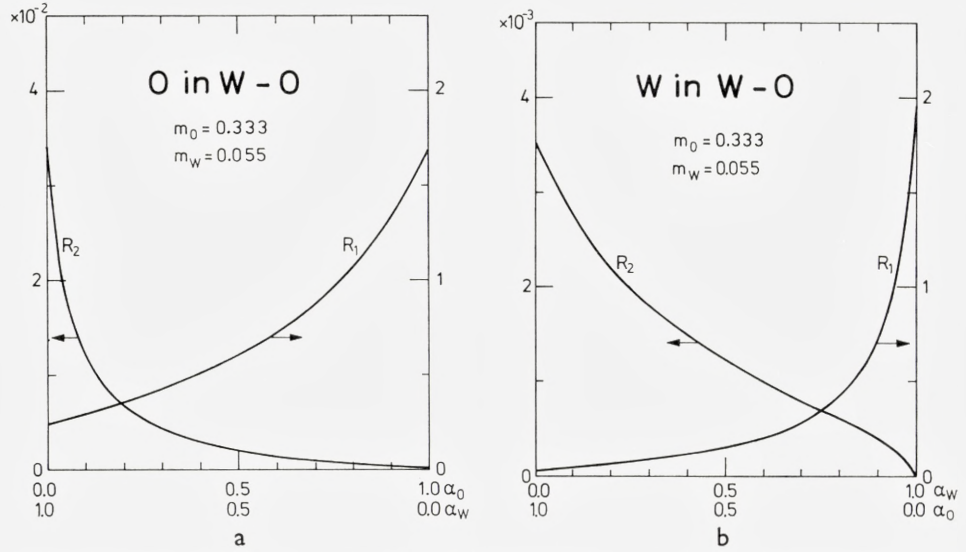

Fig. 8. First-order corrections to the slowing-down density due to atomic binding, defined in eq. (B7).

Fig. 8a. Oxygen in *W-O* compound (Index (1) refers to oxygen). Note the different scales for R_1 and R_2.

Fig. 8b. Tungsten in *W-O* compound (Index (1) refers to tungsten). Note the different scales for R_1 and R_2.

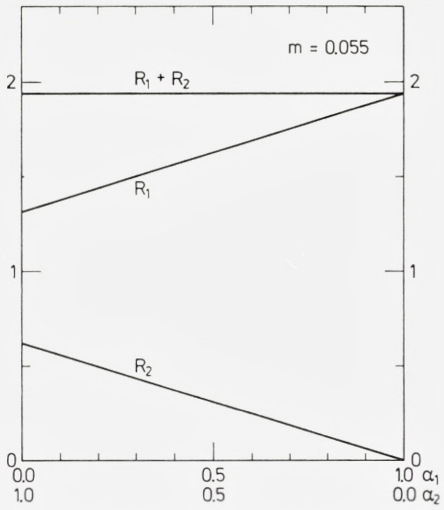

Fig. 8c. Equal-mass compound. Same scale for R_1 and R_2.

Figs. 8a and 8b indicate that the dominating contribution to eq. (B7) is due to the fact that moving atoms cannot be observed at their initial recoil energy, but at most at the recoil energy minus their respective binding energy. The loss of energy during recoiling of former generations of atoms in the cascade appears to be of minor significance for the slowing-down density.

Fig. 8c shows a similar graph for an equal-mass compound. Because of the possibility of complete exchange of energy between collision partners 1 and 2, the coefficient R_2 in (B7) becomes significant, though still smaller than R_1.

Figs. 8a–c are representative for most situations of practical interest. We conclude that the influence of atomic binding on the slowing-down density is essential only for nearly pure materials in case of very different masses, and roughly independent of concentration in case of nearly equal masses. The correction cannot exceed that of the pure material, except when the binding energies themselves undergo substantial changes due to the presence of the alloyed material.

It follows from (B7) that the influence of atomic binding is most pronounced near threshold ($E_0 \sim V_1$). In radiation damage one often meets a situation where $E_{d,i} \gg V_i$, so that the correction is unappreciable at all energies of practical interest. Therefore, we only evaluated the correction in case of the slowing-down density. In sputtering, the threshold energy of interest is the surface binding energy, which may well be comparable to V_1, so that a correction may be necessary in the lowest parts of the spectrum. Figs. 8a, b indicate that for the *W-O* system at intermediate concentrations, the correction is larger for oxygen than for tungsten. Since the sign is negative (eq. B7), the corrections tend to move the deviation from stoichiometric behaviour towards dominance of the *heavy* species in the particle flux.

References

0. N. Andersen, P. Sigmund, Atomic Collisions in Solids (B. Appleton, S. Datz, & C.D. Moak, Eds.), Plenum Press, New York (1974).
1. P. Sigmund, Rev. Roum. Phys. **17**, 823, 969, 1079 (1972).
2. J. Lindhard, V. Nielsen, M. Scharff, P. V. Thomsen, Mat. Fys. Medd. Dan. Vid. Selsk. **33**, no. 10 (1963).
3. J. Lindhard, ibid. **34**, no. 14 (1965).
4. T. Asada, K. Quasebarth, Z. Phys. Chem. *A***143**, 435 (1929).
5. G. J. Ogilvie, Aust. J. Phys. **13**, 402 (1959).
6. E. Gillam, J. Phys. Chem. Sol. **11**, 55 (1959).
7. G. S. Anderson, J. Appl. Phys. **40**, 2884 (1969).
8. W. T. Ogar, N. T. Olson, H. P. Smith, J. Appl. Phys. **40**, 4997 (1969).
9. M. L. Tarng, G. K. Wehner, J. Appl. Phys. **42**, 2449 (1971); ibid. **43**, 2268 (1972).
10. R. Kelly, N. Q. Lam, Rad. Eff. **19**, 39 (1973).
11. S. D. Dahlgren, E. D. McClanahan, J. Appl. Phys. **43**, 1514 (1972).
12. L. Q. Nghi, R. Kelly, Can. J. Phys. **48**, 137 (1970).
13. H. H. Andersen, H. Bay, Rad. Eff. **13**, 67 (1972).
14. G. K. Wehner, D. J. Hajicek, J. Appl. Phys. **42**, 1145 (1971).
15. P. Sigmund, J. Mater. Sci. **8**, 1545 (1973).
16. J. Farren, W. J. Scaife, AERE Harwell Report, R5717 (1968).
17. S. P. Wolsky, E. J. Zdanuk, D. Shooter, Surf. Sci. **1**, 110 (1964).
18. H. E. Schiøtt, Can. J. Phys. **46**, 449 (1968).
19. J. B. Sanders, Can. J. Phys. **46**, 455 (1968).
20. K. B. Winterbon, P. Sigmund, J. B. Sanders, Mat. Fys. Medd. Dan. Vid. Selsk. **37**, no. 14 (1970).
21. E. M. Baroody, Phys. Rev. **112**, 1571 (1958).
22. R. M. Felder, J. Phys. Chem. Sol. **28**, 1383 (1967).
23. M. D. Kostin, J. Appl. Phys. **37**, 3801 (1966).
24. K. B. Winterbon, Rad. Eff. **13**, 215 (1972).
25. K. B. Winterbon, J. Nucl. Sci & Eng. **53**, 261 (1974).
26. J. Kistemaker, F. J. de Heer, J. Sanders, C. Snoek, *in* Radiation Research 1966; p. 68; North-Holland Publ. Comp., Amsterdam (1967).
27. P. Sigmund, Appl. Phys. Lett. **14**, 114 (1969).
28. P. Sigmund, Phys. Rev. **184**, 383 (1969).
29. J. Lindhard, V. Nielsen, Mat. Fys. Medd. Dan. Vid. Selsk. **38**, no. 9 (1971).
30. J. Lindhard, P. V. Thomsen, *in* Radiation Damage in Solids. I., IAEA, Vienna, p. 65 (1962).

31. J. Lindhard, V. Nielsen, M. Scharff, Mat. Fys. Medd. Dan. Vid. Selsk. **36**, no. 10 (1968).
32. H. H. Andersen, P. Sigmund, Nucl. Inst. Meth. **38**, 238 (1965); Danish A.E.C., Risö Report **103** (1965).
33. M. T. Robinson, Phil. Mag. **12**, 741 (1965).
34. P. Sigmund, Rad. Eff. **1**, 15 (1969).
35. P. Sigmund, Theory of Sputtering, II (to be published).
36. G. H. Kinchin, R. S. Pease, Rep. Prog. Phys. **18**, 1 (1955).
37. J. W. Mayer, L. Eriksson, J. A. Davies, Ion Implantation in Semiconductors, Academic Press, New York (1970).

Physical Laboratory II
H. C. Ørsted Institute
DK–2100Copenhagen Ø

Indleveret til Selskabet den 29. oktober 1973.
Færdig fra trykkeriet den 12. september 1974.